U N I V E R S I T Y O F H A W A I ‘ I A T M Ā N O A
Institute for Astronomy

Pan-STARRS Project Management System

The PS-1 Lens Mount Designs

Carole Hude
Telescope Engineer
University of Hawaii
27 March 2006

PSDC-300-024-00

Revision History

Version/Revision	Date	Comments
DR		Creation of report
00		Release of report
300-024-00	27 March 2006	Changed PSDC Number

Table of Contents

List of Figures

List of Tables

1 Scope of Document

This document presents the athermalization process of the PS-1 corrector lenses, for which we consider the NOADC-M-1.0 optical design. The study has been started when the lenses design was not yet finalized, which led to some additional analyses with the final lenses designs. Some calculations considering the effect of gravity will also be performed to compare both temperature and gravity effects on stresses and displacements of the correctors. And in the case of the Dewar window, the atmospheric pressure lens distortions will be investigated.

2 Referenced Documents

Table 1. PSDC Documents

Pan-STARRS ID	Title	Authors
PSDC-300-011-01	The PS1 Telescope Image Budget Allocations	Morgan, Siegmund
PSDC-300-012-00	FEA Study of L2 Gravity Distortions	Morgan
PSDC-300-013-00	FEA Study of L3 Distortions from Atmospheric Pressure	Morgan
PSDC-300-019-DR	The PS-1 Telescope Collimation Procedure	Morgan

Table 2. External Documents

Source Reference	Title	Authors
Proceeding of SPIE, vol. 4771, Optomechanical Design and Engineering 2002, pp. 287-295	Athermal design of nearly incompressible bonds	Doyle, Michels, Genberg
	Finite element modeling of nearly incompressible bonds	Michels, Genberg, Doyle
	Springy Finite Elements Model Elastomers	Finney
SPIE, vol. 3355, March 1998	Mounting large lenses in wide-field instruments for the converted MMT	Fata, Fabricant
SPIE Press	Mounting Optics in Optical Instruments	Yoder
University of California UCO/Lick Oservatory Technical Report No. 79	The design and assembly of camera lens cells for fluid couplants using elastomeric lens mounts	Faber, Hilyard, James, Pfister
http://www.dowcorning.com	RTV 3112 Product Data Sheet	

3 Introduction

The telescope operates at temperatures between -10 °C and +30 °C, and the coefficients of thermal expansions (CTE's) of steel (and a fortiori Aluminum) and Fused Silica being very different, this would result in the generation of high stresses in the glass, not only deforming the radius of curvature of the glass, but endangering the glass itself: crack generation.

A method to reduce the thermal generated stresses in the glass consists of "potting" the glass in the cell by means of an RTV (Room Temperature Vulcanizing). These elastomers cure into flexible, form-fitting masses with reasonably good adherence properties.

The present document presents this athermalization process for the PS-1 correctors, also investigating the gravity and atmospheric pressure cases, where they apply.

4 Athermalization Design

Property	Value	Units
Elastic Modulus	7.3×10^4	N/mm^2
Poisson's ratio	0.2	-
Shear Modulus	2.8022×10^4	N/mm^2
Thermal Expansion Coefficient	1.0×10^{-6}	**/°C**
Density	2.2×10^{-3}	g/mm^3

Table 3. Assumed Physical Properties of Fused Silica

For information, Table 4 presents the physical dimensions of the three PS-1 correctors as they were considered in this study:

	Radius [mm]	Radius of curvature A surface [mm]	Radius of curvature B surface [mm]	Thickness at center [mm]
L1	318.0	892.0	977.0	104.57
L2	295.0	491.0	427.0	53.43
L3	265.0	-611.0	-569.0	40.0

Table 4. PS-1-no-ADC-M-1.0 correctors design

The primary mirror cell being made out of steel, the Upper Cassegrain Core metallic parts will be made in Steel (Carbon steel) in order to reduce the effect of temperature changes. L3 being the Dewar window, its cell will be connected to the rest of the camera's Auntie Chamber. The other camera components being made in Aluminum, the L3 cell will also be made in Aluminum.

4.1 Athermalization Process – Closed-form equations

For the detailed athermalization procedure, see Appendix 1. The data necessary for the determination of the optimal RTV thickness are the optics radii (see Table 4) and the RTV, glass and metals physical properties (see Table 5)

The elastomer data is taken from Yoder, for RTV3112 (RTV Silicone Rubber) from Dow Corning:

Physical property	Symbol	Value
Elastomer Young's Modulus	E_{bond}	3.447 MPa
Elastomer coefficient of thermal expansion	α_{bond}	300.6 x 10^{-6} /°C
Elastomer Poisson's ratio	ν_{bond}	0.499
Optics coefficient of thermal expansion	α_{optic}	1 x 10^{-6} /°C
Cell coefficient of thermal expansion (steel)	α_{cell}	13 x 10^{-6} /°C
Cell coefficient of thermal expansion (Aluminum)	α_{cell}	24 x 10^{-6} /°C

Table 5. Physical properties of materials used in the athermalization design

	"Athermal" RTV thickness [mm]
L1	4.374
L2	4.05
L3	7.167

Table 6. Athermal RTV thickness for PS-1 correctors

4.2 Preliminary athermalization studies on L2

According to Yoder the biconvex lens shape gives the highest stresses compared to other lens shapes, for the same RTV thickness. We will therefore proceed to some preliminary studies on the second corrector in order to determine if the RTV thickness derived from the closed-form equation indeed gives us low stresses.

The reference temperature is considered to be 24 °C, the room temperature at which the assembly will be performed.

We consider two thermal load cases: the first one at the lowest expected operating temperature (-10 °C) and the second at the highest expected temperature (+30 °C). Two different designs are considered: one with the RTV ring reaching the cell bottom surface, and one leaving a space between the RTV ring and the cell bottom surface, to allow for thermal expansion and contraction of the RTV free surfaces.

We calculate only a quarter model for improving the calculation time, taking advantage of the model symmetry. The lower surface of the cell is constrained in axial displacements: cell simply supported. For the modeling we try to force Cosmos to add as many elements through the RTV thickness, as recommended by Michels et al.

The Von Mises stresses in the glass are presented in Figure 1 to Figure 4, and the main results summarized in Table 7.

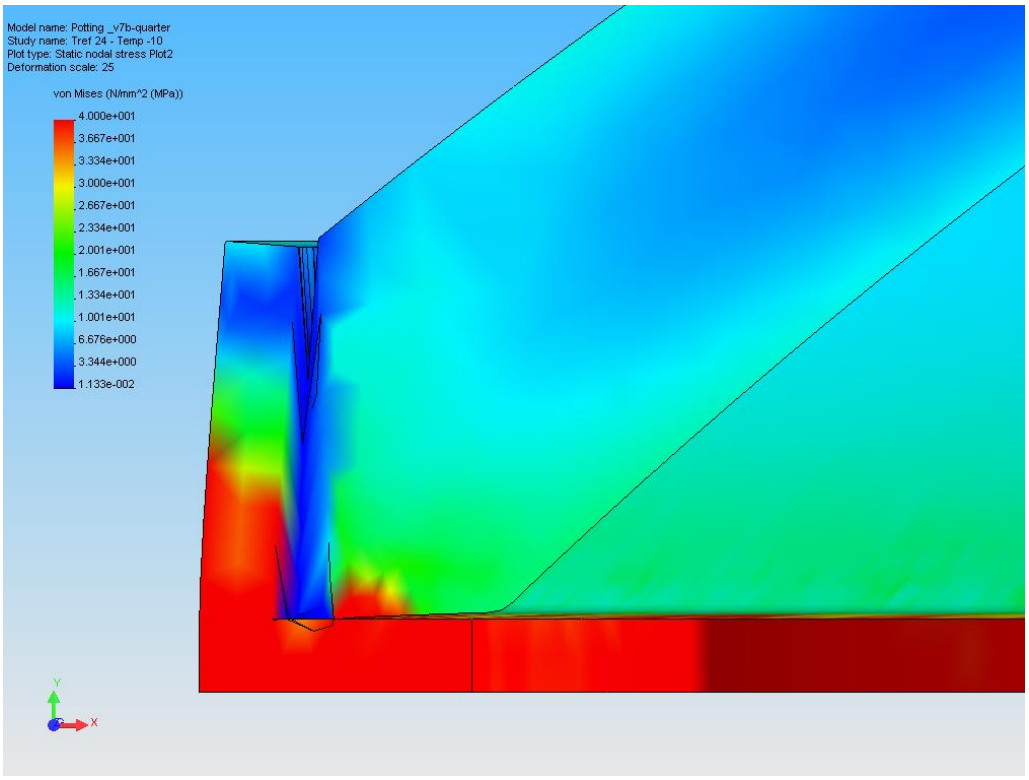

Figure 1. RTV Ring down to the cell bottom surface – T = -10 °C Von Mises Stresses – Modified scale to visualize stresses in the glass

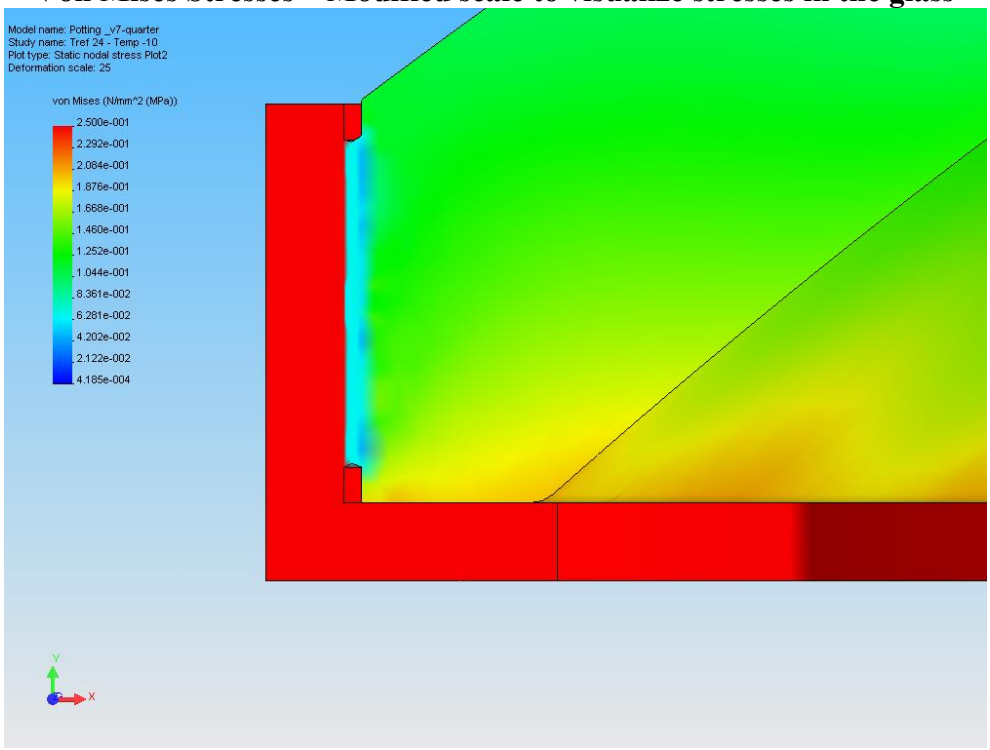

Figure 2. RTV Ring on the center of the external glass rim – T = -10 °C Von Mises Stresses – Modified scale to visualize stresses in the glass

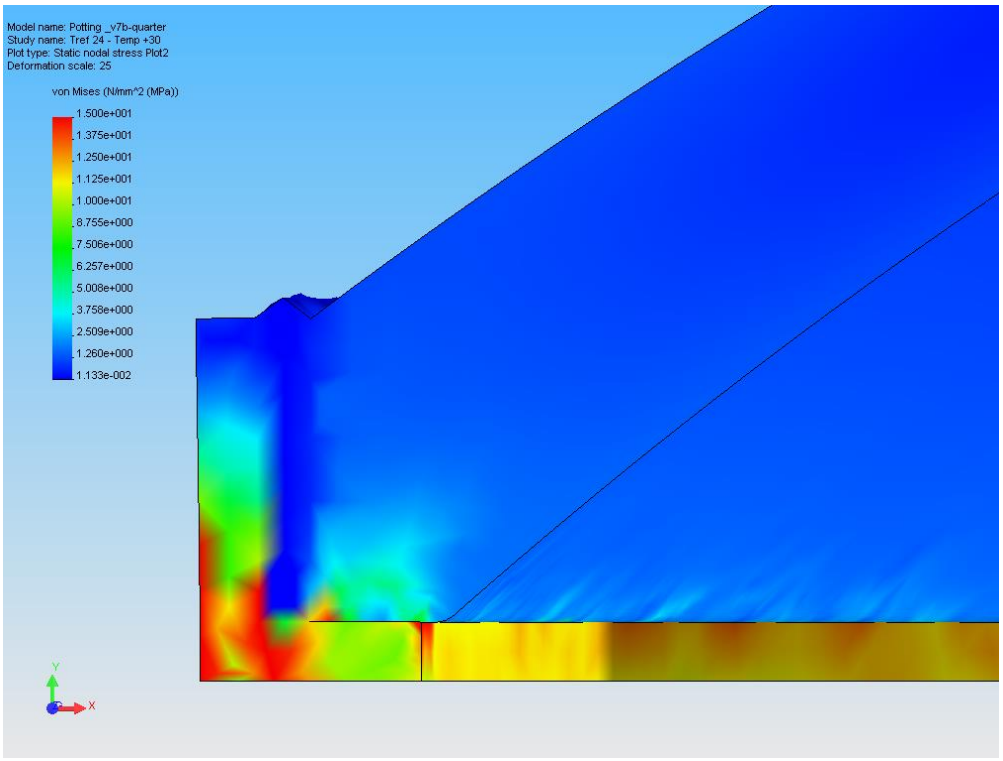

Figure 3. RTV Ring down to the cell bottom surface – T = +30 °C Von Mises Stresses – Modified scale to visualize stresses in the glass

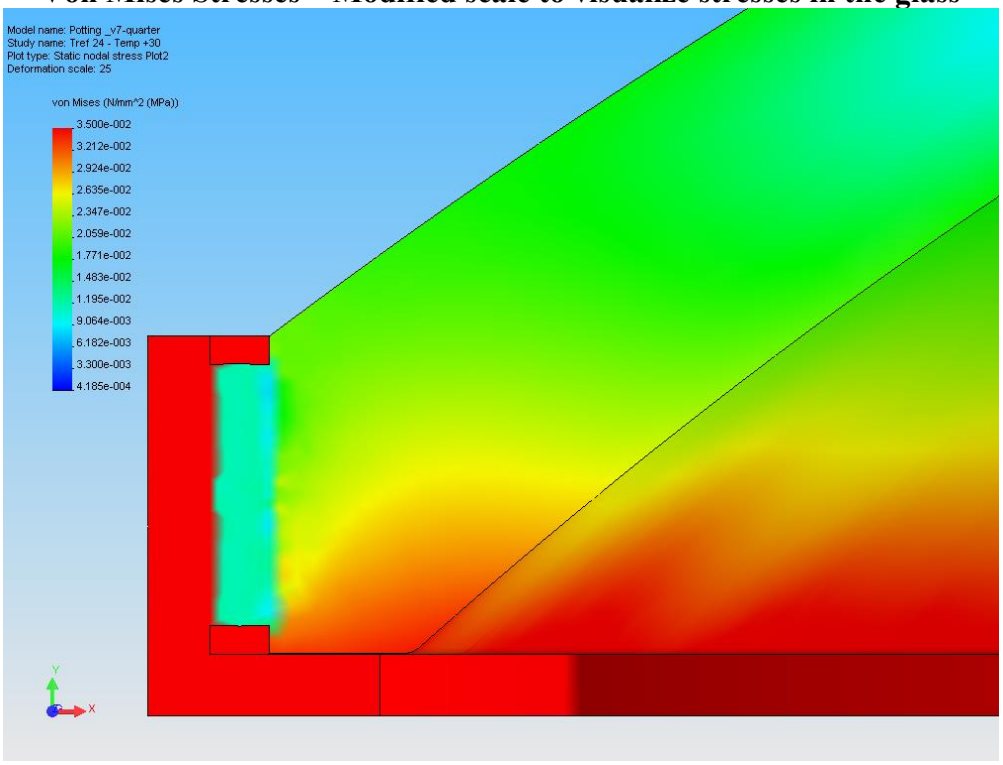

Figure 4. RTV Ring on the center of the external glass rim – T = +30 °C Von Mises Stresses – Modified scale to visualize stresses in the glass

		RTV ring down to the cell	RTV ring with space left to cell
T = -10 °C (ΔT= 34 °C)	Max. stress (σ_{max}) on lens surfaces	21.9 MPa [3,181 psi]	0.21 MPa [31 psi]
	Max stress inside the glass	98 MPa [14,214 psi]	0.24 MPa [34 psi]
	Axial disp. at lens vertex	56.5 μm (L2A) 56.9 μm (L2B)	-5.3 μm (L2A) -4.8 μm (L2B)
	Max. radial disp	148.1 μm	132.6 μm
	Exact solution (contraction) $\Delta R=\Delta T x \alpha_{cell} x R_{cell}$	134 μm	
T = +30 °C (ΔT= 6 °C)	Max. stress (σ_{max}) on lens surfaces	3.9 MPa [566 psi]	0.24 MPa [35 psi]
	Max stress inside the glass	14.5 MPa [2,109 psi]	0.034 MPa [5 psi]
	Axial disp. at lens vertex	-7.3 μm (L2A) -7.4 μm (L2B)	1.8 μm (L2A) 1.7 μm (L2B)
	Max. radial disp	-24.8 μm	-23.4 μm
	Exact solution (expansion)	-23.7 μm	

Table 7. Preliminary atermalization study results

These analyses indicate that some space needs to be provided between the RTV ring and the lens cell bottom surface, in order to leave some room for the RTV to contract and expand freely. The thickness that has been considered here corresponds to the value derived from the closed-form equations, for the case of L2. The space left between RTV and cell is of about 2 mm, but the RTV only expands a small fraction of these 2 mm.

Concerning the radial displacements obtained with the partial RTV ring, the discrepancy with respect to the exact solution is only of about 1%.

Yoder modeled in his book a similar problem with a smaller and thinner lens: a 52.095 mm diameter Germanium lens. The biconvex lens shape gives the highest stresses in the glass, including for the athermal thickness. This athermal thickness is determined with the Bayer equation, shown in Appendix 1 to be the least accurate of the three equations. The resulting stress in the glass for this athermal thickness and this lens shape, is 108 psi, whereas when using an RTV thickness 7.7 times smaller (0.01 in. vs 0.077 in.), the stress in the glass reached 787 psi.

5 PS-1 correctors FEA results

5.1 First corrector (L1)

The previous results are now applied to the first corrector lens design. The closed-form equations give an RTV thickness of 4.374 mm. The same mesh size is used in this model as for the preliminary athermalization study, namely 10 mm.

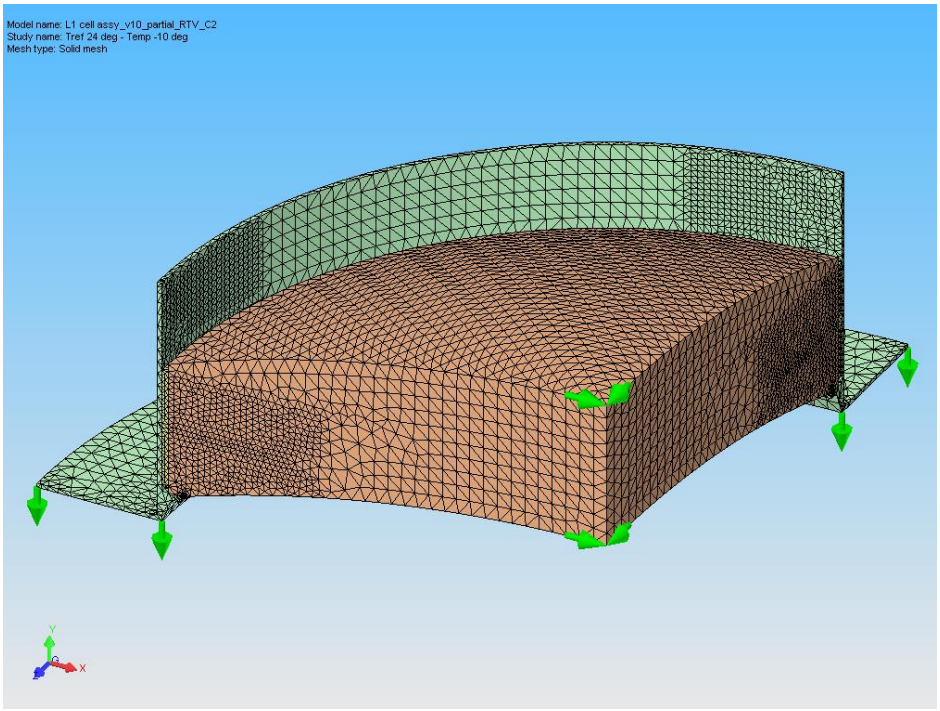

Figure 5. L1 cell quarter model mesh and boundary conditions

5.1.1 Temperature effect

We consider the same two thermal load cases as before. The results obtained with this model are presented in Figure 6 and Figure 7, and are summarized in Table 8.

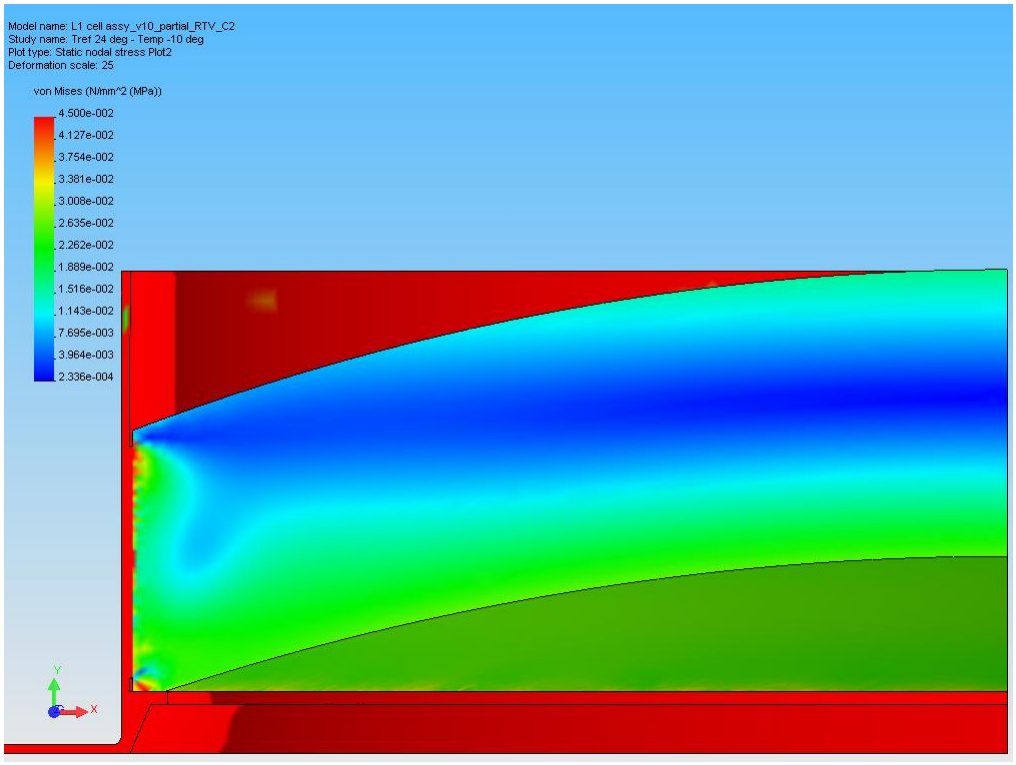

Figure 6. T = -10 °C - Von Mises Stresses – Modified scale to visualize stresses in the glass

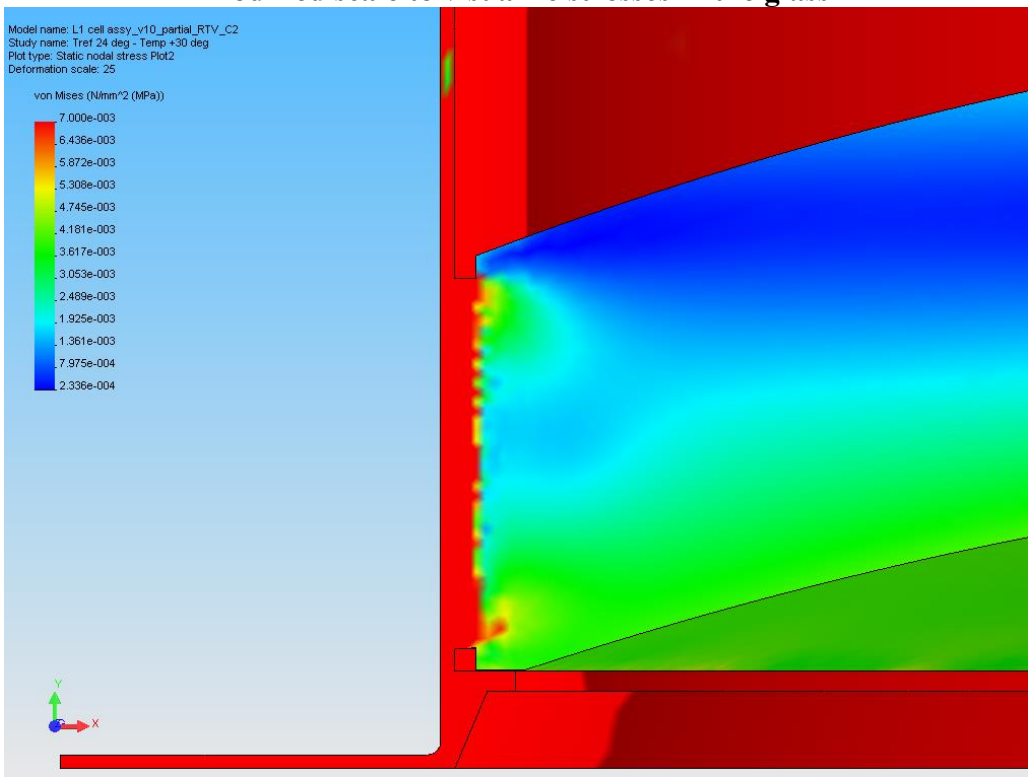

Figure 7. T = +30 °C -Von Mises Stresses – Modified scale to visualize stresses in the glass

		L1 cell t_e=4.374 mm
T = -10 °C (ΔT= 34 °C)	Max. stress (σ_{max}) on lens surfaces	0.035 MPa [5 psi]
	Max stress inside the glass	0.05 MPa [8 psi]
	Axial disp. at lens vertex	-15.0 μm (L1A) -11.4 μm (L1B)
	Axial disp. of the lens perimeter	-13.2 μm (L1A) -10.0 μm (L1B)
	Max. radial disp	182.8 μm
	Exact solution (contraction) $\Delta R=\Delta T x \alpha_{cell} x R_{cell}$	182.4 μm
T = +30 °C (ΔT= 6 °C)	Max. stress (σ_{max}) on lens surfaces	0.005 MPa [0.7 psi]
	Max stress inside the glass	0.009 MPa [1.3 psi]
	Axial disp. at lens vertex	6.1 μm (L1A) 5.5 μm (L1B)
	Axial disp. of the lens perimeter	5.8 μm (L1A) 5.2 μm (L1B)
	Max. radial disp	-32.16 μm
	Exact solution (thermal expansion)	- 32.2 μm

Table 8. FEA Results on L1 cell

5.1.1.1 Sensitivity study on the RTV thickness

In order to obtain a rounded radius value in inches for the lens cell, we define the internal radius of the L1 cell to be 12.69 inches (322.326 mm) which gives an elastomer ring thickness of 4.326 mm.

We then investigated how the manufacturing tolerances on both the metal cell and the glass would affect the athermalization of the lens. Considering a tolerance of 0.005 in., we would have a radius of either 12.685 in. (322.199 mm) or 12.695 in. (322.453 mm), yielding an RTV thickness of either 4.199 mm (-4%) or 4.453 mm (+1.8%). But if we consider a similar tolerance on the glass itself, we would end up with an inner radius of either 12.68 in. (322.072 mm) or 12.7 in. (322.58 mm), finally yielding an RTV thickness of 4.072 mm (-6.9%) or 4.58 mm (+4.7%).

The first additional FEA analyses we performed show us that the worst case is always the -10 °C load case, so we will limit our analyses to this load case, to limit the number of calculations to be performed. These results are summarized in Table 9 and the complete sensitivity analysis is presented in Figure 8.

The “nominal” RTV thickness of 4.326 mm is not calculated: we assume that there is enough data for the resulting graph to be accurate.

		L1 cell t_e=4.199 mm	**L1 cell t_e=4.374 mm**	**L1 cell t_e=4.58 mm**
T = -10 °C (ΔT= 34 °C)	Max. stress (σ_{max}) on lens surfaces	0.2 MPa [29 psi]	0.035 MPa [5 psi]	0.15 MPa [21 psi]
	Max stress inside the glass	0.29 MPa [41 psi]	0.05 MPa [9 psi]	0.73 MPa [105 psi]
	Axial disp. at lens vertex	-13.7 µm (L1A) -10.1 µm (L1B)	-15.0 µm (L1A) -11.4 µm (L1B)	-16.2 µm (L1A) -11.6 µm (L1B)
	Axial disp. of the lens perimeter	-12.6 µm (L1A) -9.4 µm (L1B)	-13.2 µm (L1A) -10.0 µm (L1B)	-13.6 µm (L1A) -10.2 µm (L1B)
	Max. radial disp	181.5 µm	182.8 µm	182.9 µm
	Exact solution (contraction) $\Delta R=\Delta T x \alpha_{cell} x R_{cell}$	182.4 µm		
T = +30 °C (ΔT= 6 °C)	Max. stress (σ_{max}) on lens surfaces	0.022 MPa [3.2 psi]	0.005 MPa [0.7 psi]	0.67 MPa [98 psi]
	Max stress inside the glass	0.028 MPa [4.1 psi]	0.009 MPa [1.3 psi]	0.02 MPa [3 psi]
	Axial disp. at lens vertex	6.0 µm (L1A) 5.4 µm (L1B)	6.1 µm (L1A) 5.5 µm (L1B)	6.2 µm (L1A) 5.6 µm (L1B)
	Axial disp. of the lens perimeter	5.8 µm (L1A) 5.3 µm (L1B)	5.8 µm (L1A) 5.2 µm (L1B)	5.7 µm (L1A) 5.2 µm (L1B)
	Max. radial disp	-32.05 µm	-32.16 µm	-32.29 µm
	Exact solution (thermal expansion)	- 32.2 µm		

Table 9. Evolution of stresses according to the RTV thickness

Some additional thicknesses are considered for obtaining a more accurate curve, but the results are not presented in Table 9.

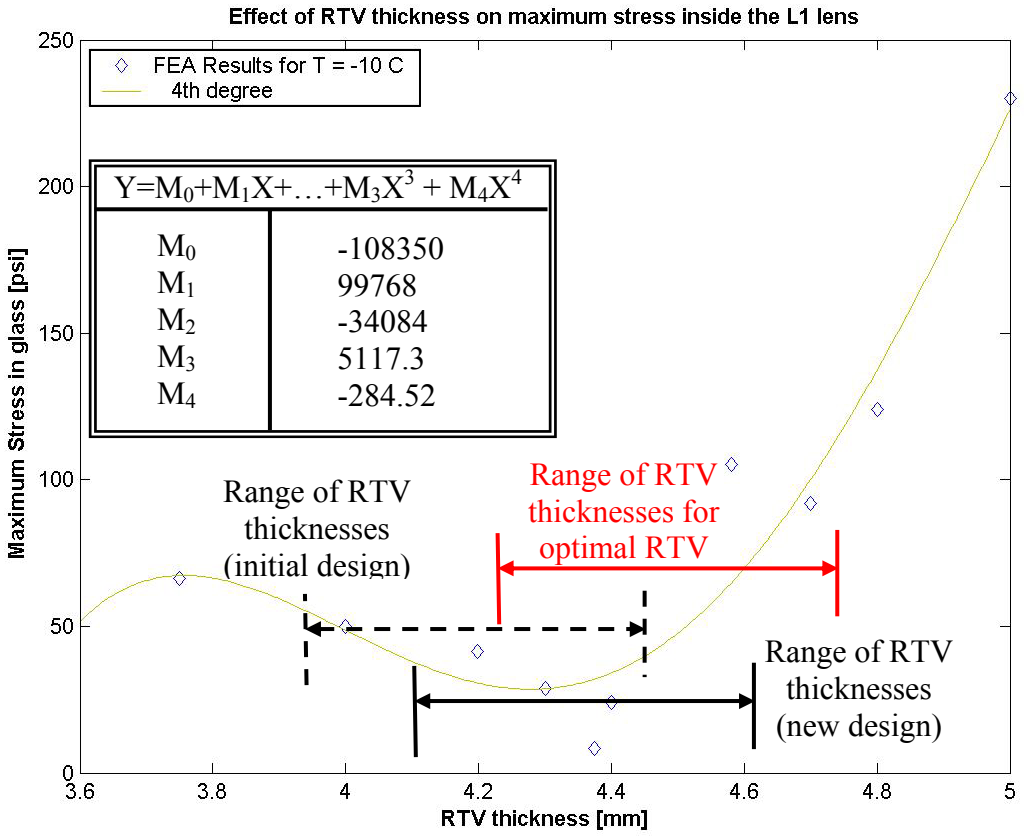

Figure 8. Evolution of stresses on and in the glass with respect to RTV thickness, at -10 degrees C

Therefore, from the above figure, we would recommend to choose the nominal RTV thickness to be slightly below the optimal RTV thickness, so that when considering a manufacturing tolerance of 0.005 in. on both the cell and the glass, the maximum stress inside the glass would be reduced by the shift to the lower side of the curve. For the initial design, this would consist of having an RTV thickness in the range [3.945 mm, 4.453 mm], giving stresses between 40 and 54 psi.

The above results are obtained for a thin lens cell and the results do not seem to be very good (when comparing to the ones obtained for L2 and L3). We therefore performed the same sensitivity study for the new L1 design, using a thicker cell: 4.7625 mm (3/16 in.) instead of the original 3.175 mm (1/8 in.): see Figure 9. The results of the new sensitivity study are presented in Figure 10.

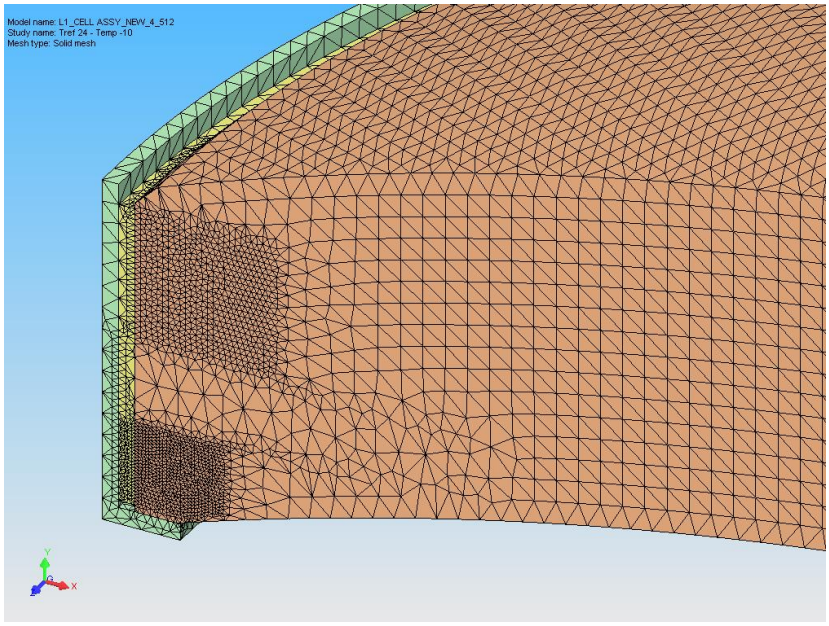

Figure 9. New L1 cell and lens designs

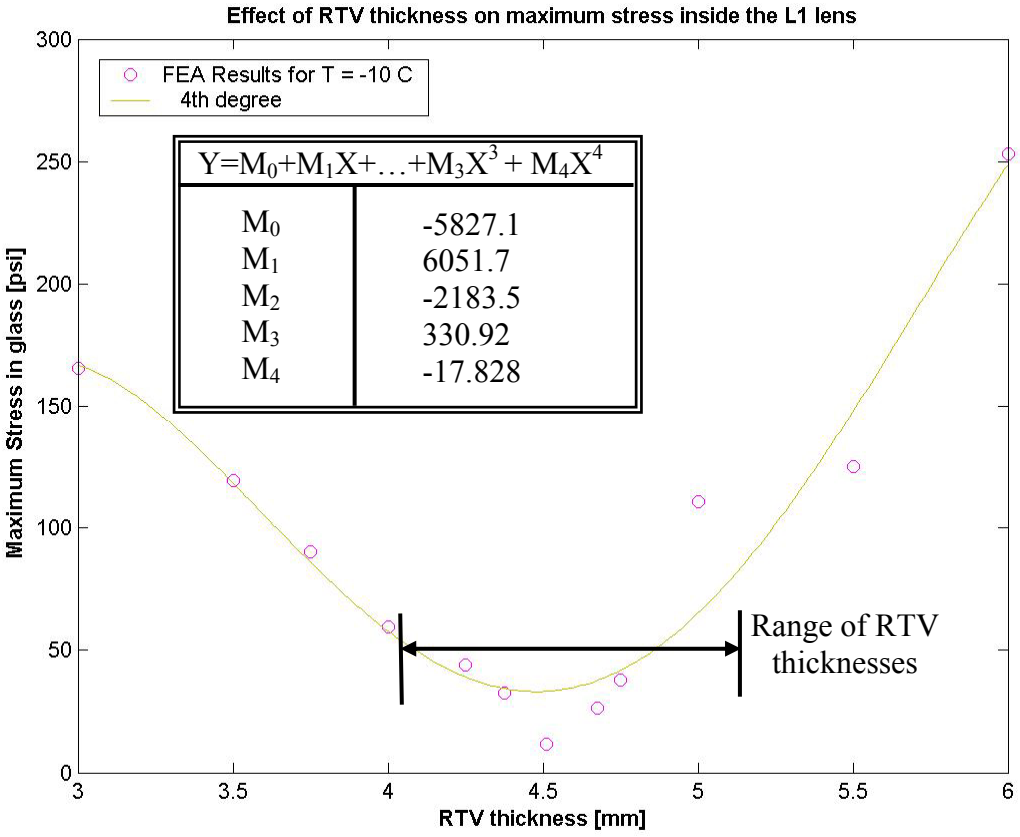

Figure 10. Evolution of stresses on and in the glass with respect to RTV thickness, at -10 degrees C for the new L1 cell and lens designs

We observe a behavior as we would have expected earlier. It therefore seems that the cell thickness should not be thinner than 3/16 in. There is no more need to aim a thinner RTV thickness.

5.1.1.2 Lens and cell not concentric

We then investigated the case when the lens and the cell are not perfectly centered. In our analysis the decentering of L1 in its cell is of 0.5 mm (ca. 0.002 in.). We considered the nominal diameter for L1 and an RTV thickness of 4.58 mm before eccentricity. As we calculate a quarter model (not representing the reality), we have an RTV thickness of 4.58 mm in -X and 4.08 mm in -Z.

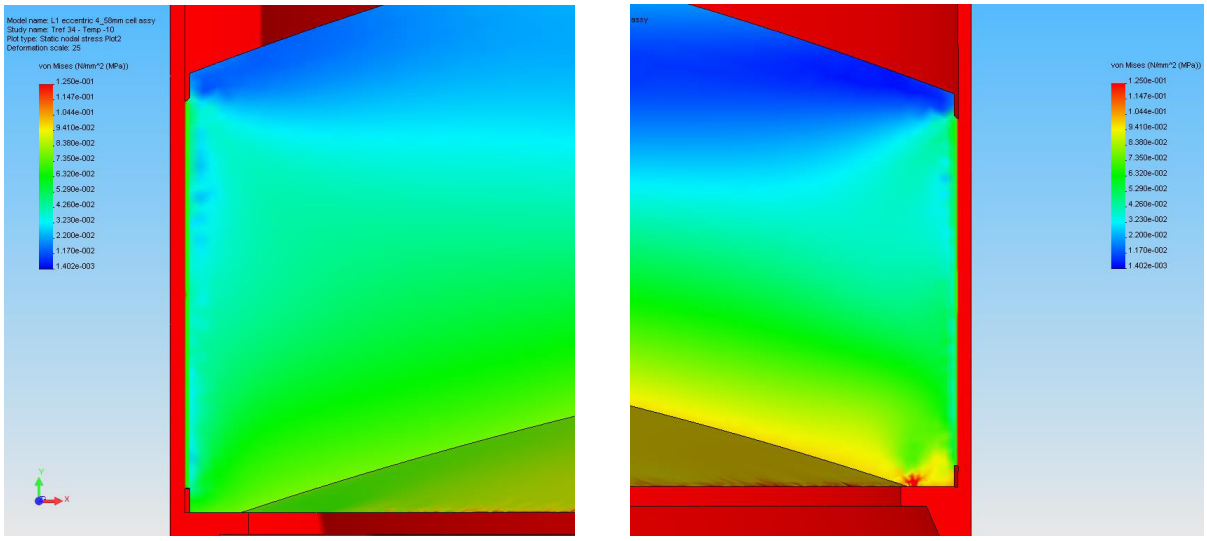

Figure 11. Stresses in a lens mounted with a decenter of 0.5 mm in its cell (the thinnest RTV thickness is shown on the right)

		L1 cell t_e=4.58 mm, lens eccentrically mounted
T = -10 °C (ΔT= 34 °C)	Max. stress (σ_{max}) on lens surfaces	0.21 MPa [31 psi]
	Max stress inside the glass (4.08 mm side)	0.49 MPa [72 psi]
	Max stress inside the glass (4.58 mm side)	0.09 MPa [13 psi]
	Axial disp. at lens vertex	-14.1 µm (L1A) -10.6 µm (L1B)
	Axial disp. of the lens perimeter	-12.8 µm (L1A) -9.6 µm (L1B)
	Max. radial disp	187.2 µm
	Exact solution (contraction) $\Delta R=\Delta T x \alpha_{cell} x R_{cell}$	182.4 µm

Table 10. FEA results for the lens mounted with a decenter of 0.5 mm in its cell

These results need to be compared with the ones obtained with the concentric RTV rings of 4.58 mm (σ_{max}=105 psi) and 4.072 mm (σ_{max}=41 psi), the closest data available, comparable to the 4.08 mm on that side of the lens. The maximum stresses in the glass are lower than the ones obtained in both cases. The difference is that the displacements and stress distribution are not symmetrical anymore.

5.1.2 Gravity Loads – De-centering at horizon

For this analysis, L1 seemed the most appropriate lens, due to its geometry. We considered the lens at horizon, in order to determine the lens de-centering due to the "squeezing" effect of the RTV under the lens weight.

Yoder gives a closed-form equation to determine this de-centering, based on the Valente and Richard equation:

$$\delta = \frac{m_{optics} g t_e}{\pi R_{optics} t_E \left[\frac{E_e}{1-\nu_e^2} + \frac{E_e}{2(1+\nu_e)} \right]} = \frac{2 m_{optics} g t_e (1-\nu_e^2)}{\pi R_{optics} t_E E_e (3-\nu_e)},$$

which for a weight of 71.2 kg for L1, and an edge thickness of 95.45 mm, gives a de-centering of 5.58 µm. The model we used was a half model, therefore the 5.58 µm previously calculated would end up in 2.79 µm.

The FEA analysis yields a de-centering of 2.1 µm at the L1A vertex and 1.8 µm at the L1B vertex, slightly smaller than the value resulting from the above equation.

The stresses generated in L1 are very small (about 10 psi), and definitely negligible with respect to the stresses generated by the temperature difference.

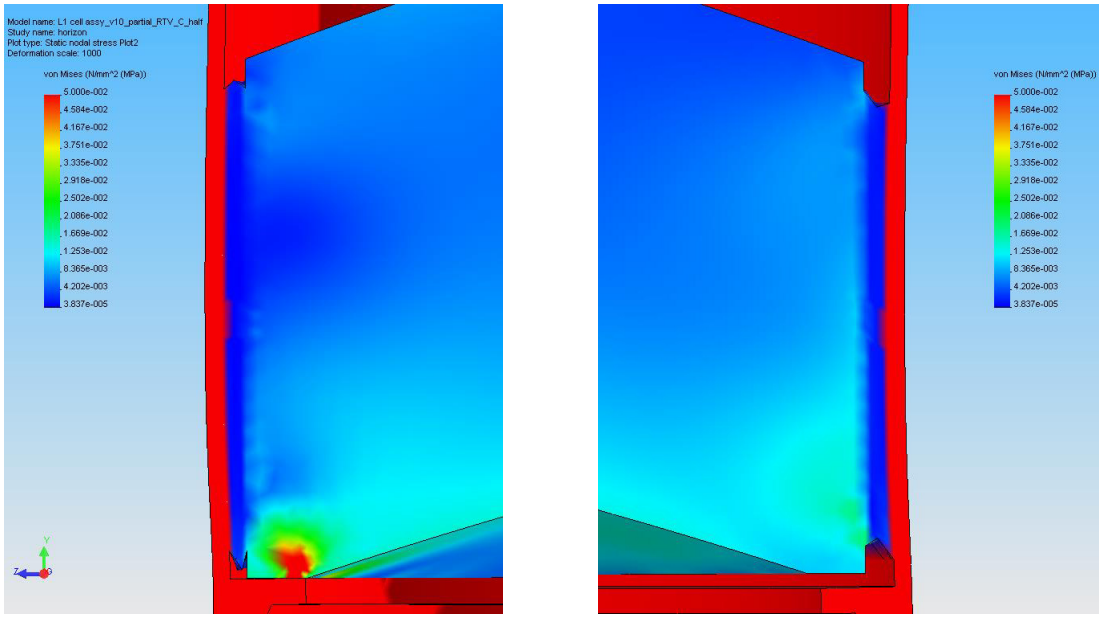

Figure 12. Stresses in L1 at horizon – RTV compressed (left side – bottom w.r.t. gravity direction) and stretched (right side – top w.r.t. gravity direction)

5.2 Second corrector (L2)

5.2.1 Temperature effect: sensitivity study on the RTV thickness

We proceed to the same sensitivity study as for L1. In the case of L2, this sensitivity study was performed when the final design of the PS-1 correctors was available. L2 has now an outer radius of 305 mm, yielding an RTV thickness of 4.195 mm.

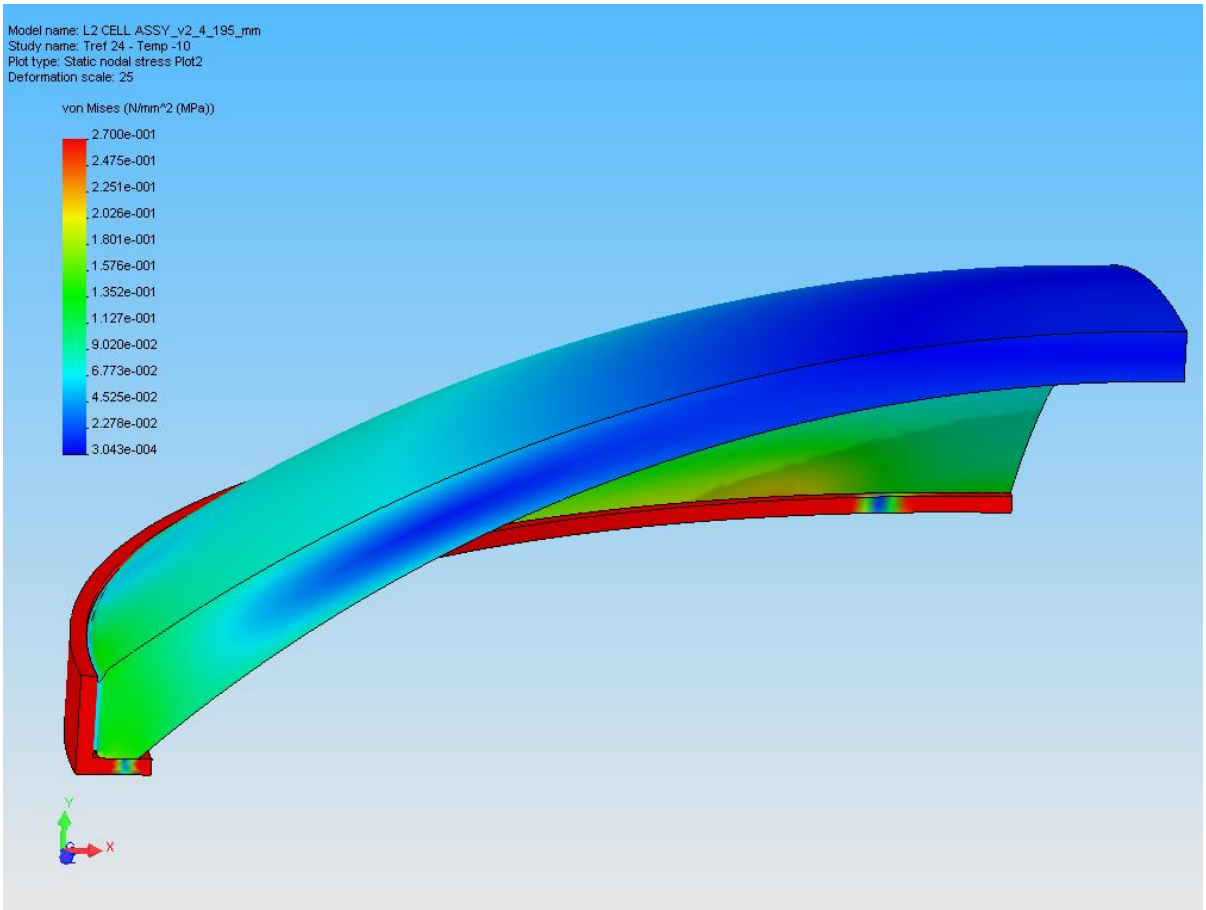

Figure 13. T = -10 °C - Von Mises Stresses – Modified scale to visualize stresses in the glass

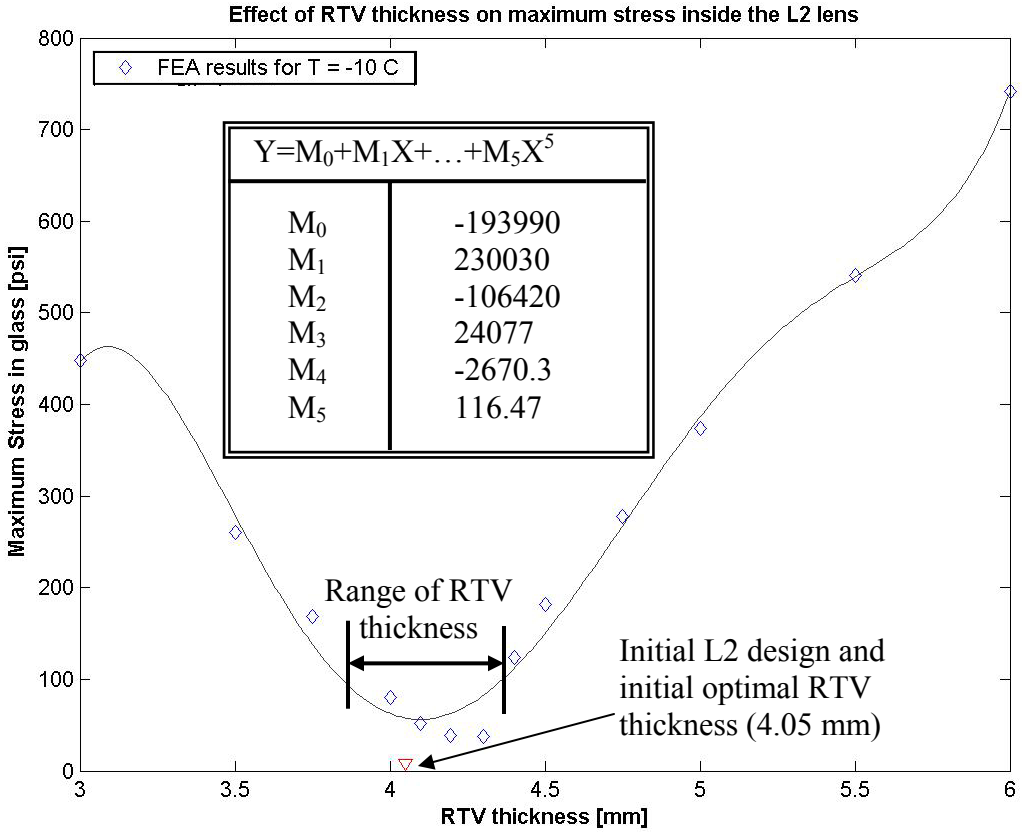

Figure 14. Effect of RTV thickness on maximum stresses in L2

The effect of the RTV thickness variation over the stresses in the glass is similar to the one obtained for L1 (new design). If we consider a rounded number, for the L2 cell inner diameter, of 12.17 in. (309.118 mm), this yields a nominal RTV thickness of 4.118 mm. When considering similar fabrication tolerances on both the cell and the lens as previously, we would end up with a minimum RTV thickness of 3.864 mm and a maximum thickness of 4.372 mm. We would therefore have stresses in the glass ranging from about 40 psi to about 41 psi, as we are in the flat portion of the curve.

5.2.2 Comparison between temperature and gravity generated stresses

Due to its shape, L2 is the most sensitive to gravity loads, so we proceeded to a final calculation considering L2 at zenith.

	Worst temperature load case T = -10 °C (ΔT= 34 °C)	**Gravity (zenith) load case**
Max. stress (σ_{max}) on lens surfaces	0.21 MPa [30 psi]	0.11 MPa [16 psi]
Max stress inside the glass	0.27 MPa [39 psi]	0.09 MPa [13 psi]
Axial disp. at lens vertex	-5.7 μm (L2A) -5.2 μm (L2B)	-0.11 μm (L2A) -0.11 μm (L2B)

Table 11. Comparison between temperature and gravity generated stresses in L2

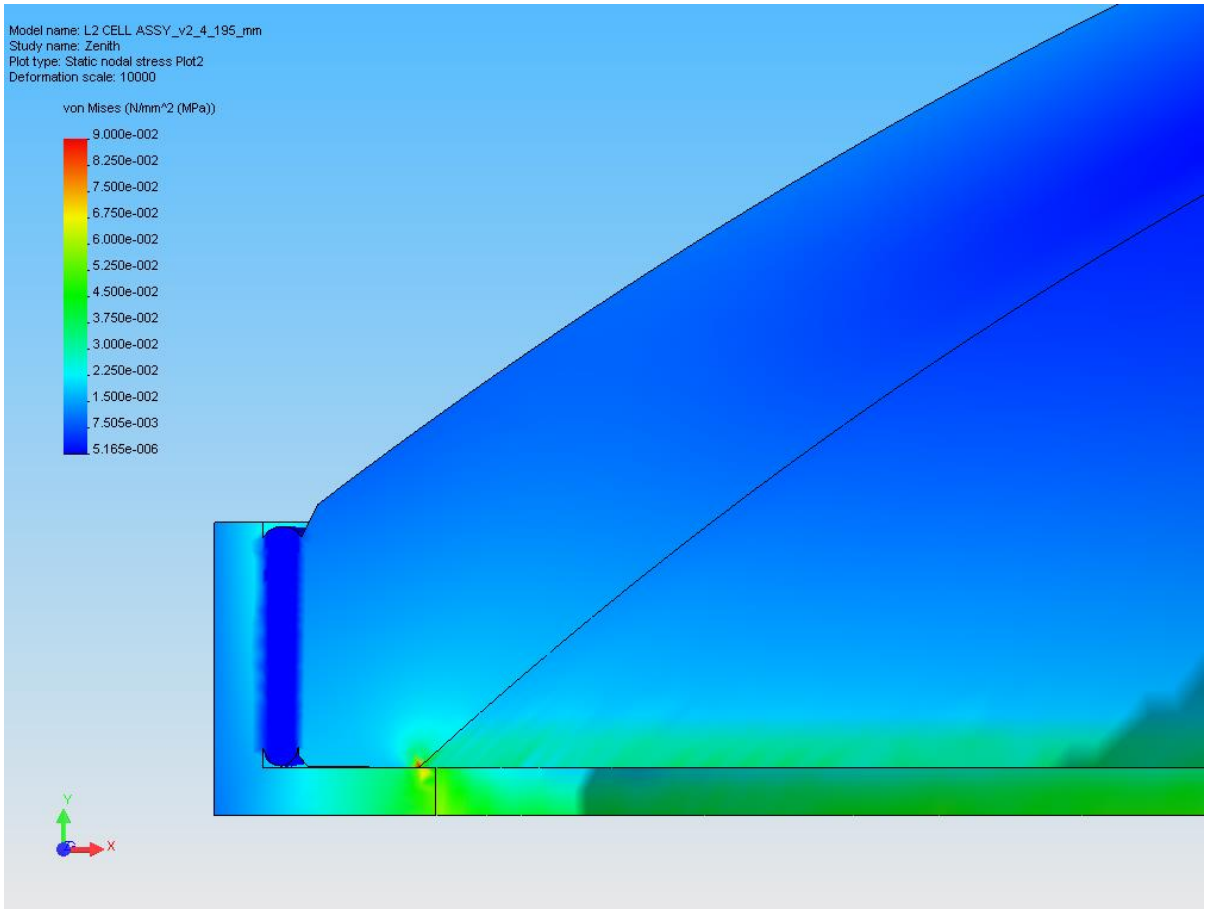

Figure 15. Stresses in L2 under gravity, at zenith

These results show that the temperature induced stresses in the lens are greater than the gravity induced ones.

The gravity induced displacements of the L2 corrector were investigated in PSDC-300-012-00, considering the lens alone and restraining the outer rim of the lens. The maximum displacement (at the L2A vertex) was found to be -3.79 x 10^{-5} mm, i.e -3.79 x 10^{-2} μm. We find with our model a maximum displacement of the L2A vertex of -0.11 μm, about a factor 3 higher. In order to clarify this, we proceeded to some additional analyses, with the design prior to the final one.

The geometry of the L2 corrector evolved slightly since PSDC-300-012-00: additional 5 mm in radius, flat surface at the bottom for mounting purposes and therefore an additional 2 mm fillet radius at the junction between flat and curved surfaces. Considering the new L2 design and applying the same boundary conditions as in PSDC-300-012-00, we obtain a maximum axial displacement of the L2A vertex of -3.74x10^{-5} mm, to be compared to the -3.79 x 10^{-5} mm of PSDC-300-012-00. Differences in the boundary conditions might explain these results discrepancies. If we keep L2 alone and simply support it on its bottom flat surface, we obtain a maximum L2A vertex displacement of -0.13 μm, much closer to what we found. If we then take the L2 cell assembly and apply the same "fixed" boundary condition on the outer rim, we still obtain -0.12 μm. The difference in results comes from the introduction of the elastomer and the possibility for the glass to slide, due to the presence of the contact elements (node-to-node) between glass and metal.

A Zemax study on the gravity generated distortions of L2 will need to be performed.

To be thorough, we also investigated the effect when pointing to horizon.

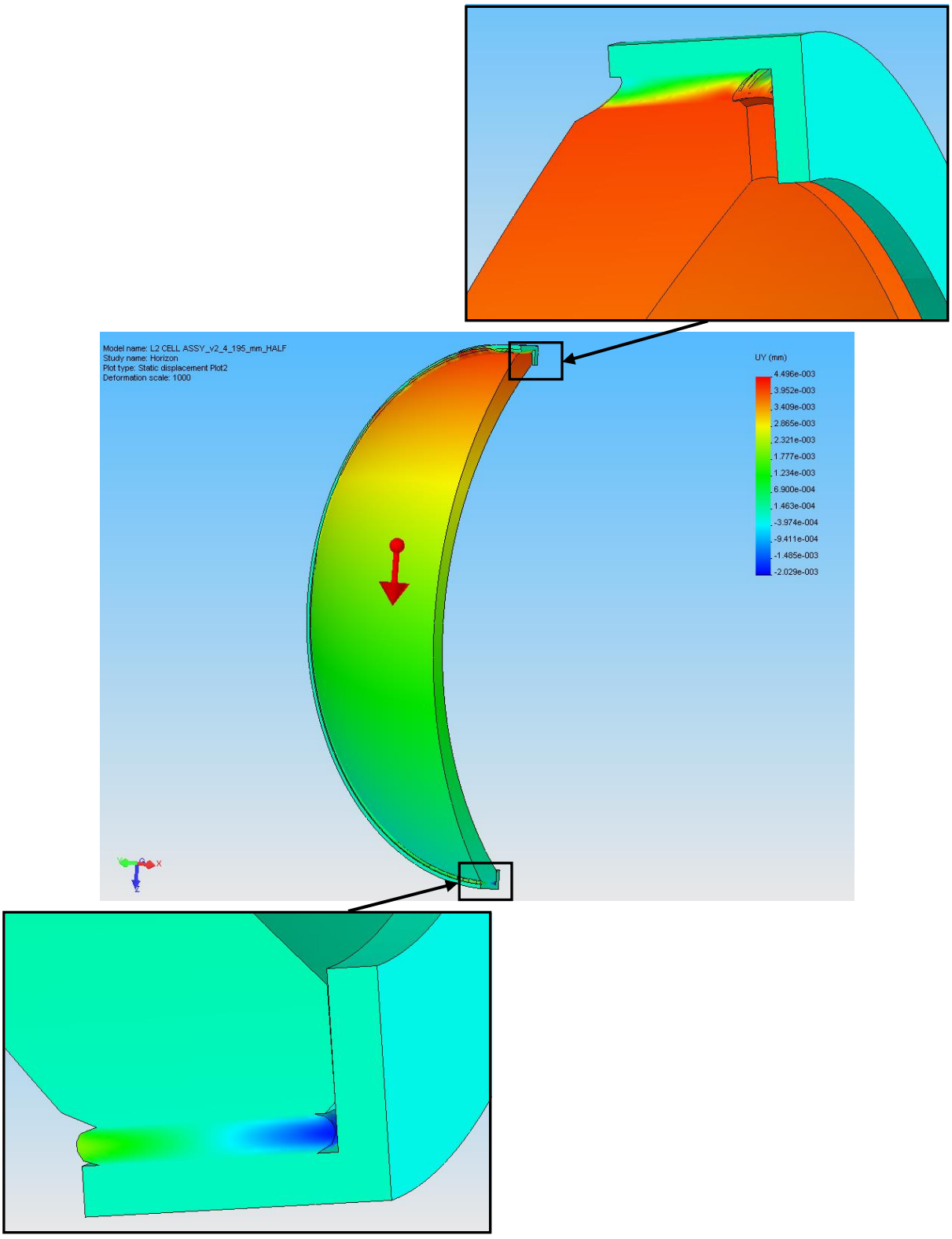

Figure 16. L2 corrector at horizon – displacements in the gravity direction (z)

We do not observe the similar behavior due to the magnitude of the displacements: in the preliminary study we observed a peak-to valley difference of 56 nm. The de-center of the L2 vertices is 1.3 µm.

5.3 Third corrector and Dewar window (L3)

5.3.1 Temperature effect

Prior to the final definition of the PS-1 corrector design, we performed a similar sensitivity analysis as for the L1 corrector. The L3 cell designed by the camera group has been slightly modified to comply with the athermal RTV thickness of 7.17 mm defined in Table 6.

We considered a uniform temperature of -10 °C (T_{ref}= 24 °C). The resulting stresses are presented in Figure 17.

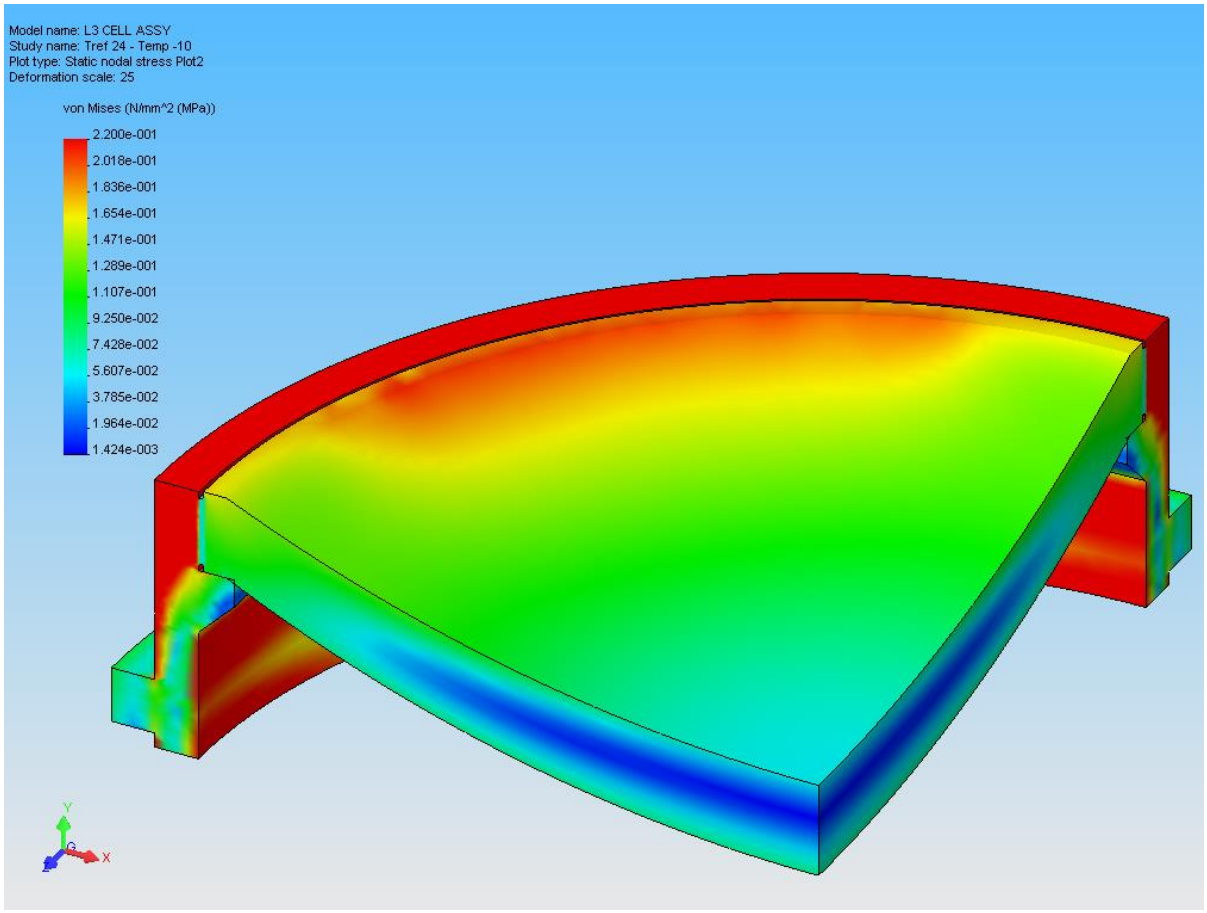

Figure 17. Von Mises Stresses in L3 for a uniform temperature of -10 °C – Scale modified for visualizing the stresses in the glass

The results of the sensitivity study are presented in Figure 18.

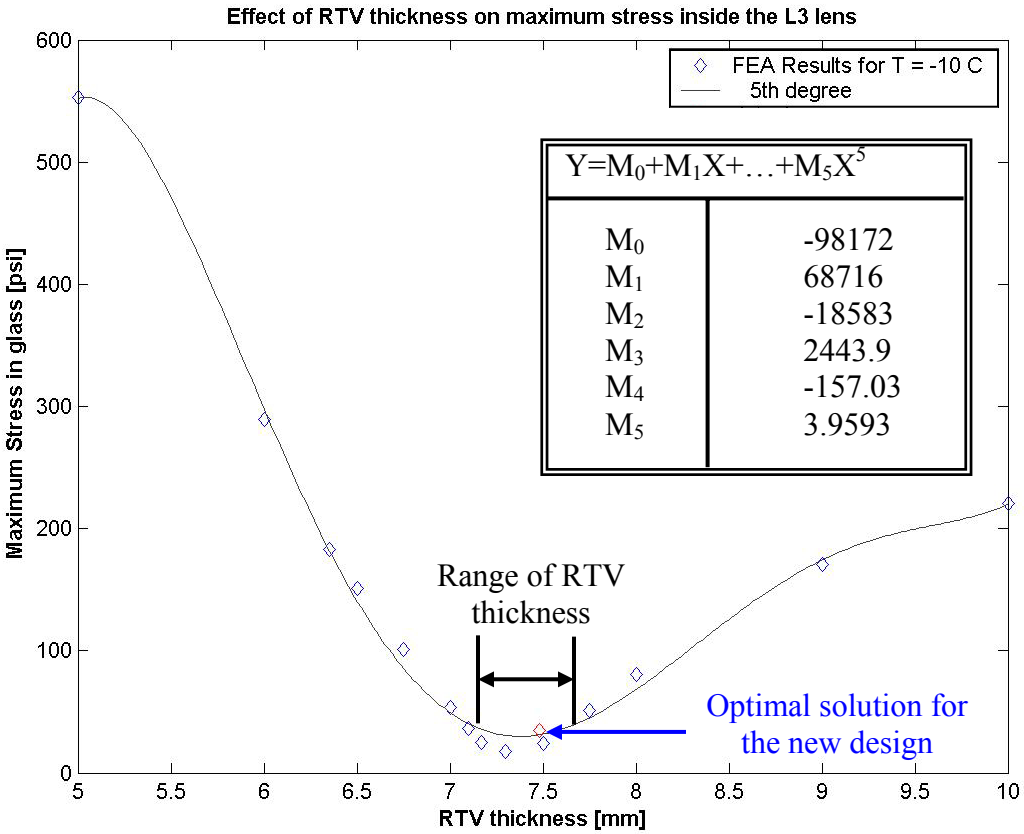

Figure 18. Effect of RTV thickness on stresses in the L3 corrector

We observe a different behavior as for the L1 and L2 correctors, due to the different shape of lenses: respectively bi-convexes and biconcave.

We performed a final calculation on the latest design of the L3 cell (diameter of 554 mm), to check stress levels:

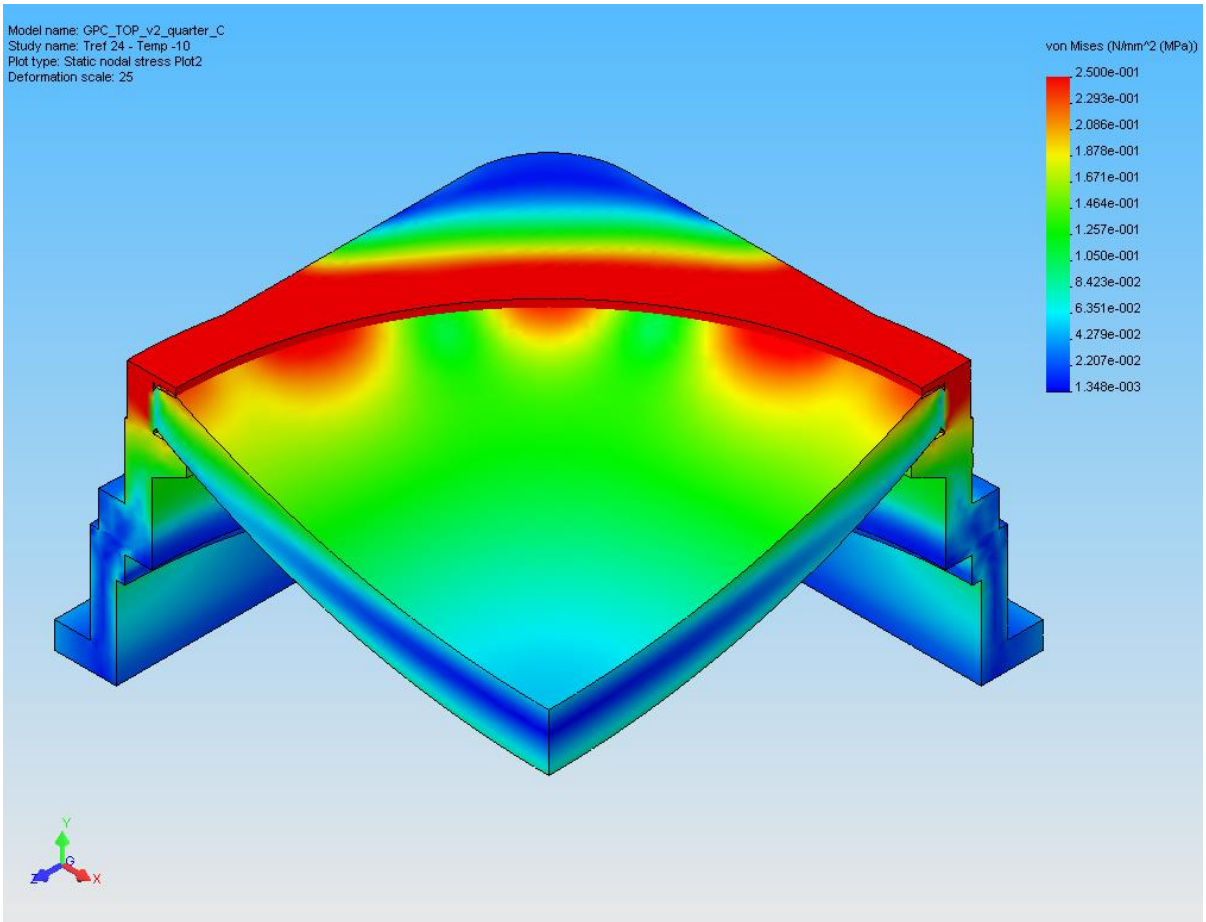

Figure 19. Von Mises Stresses in L3 (new design) for a uniform temperature of -10 °C – Scale modified for visualizing the stresses in the glass

The maximum stress in L3 is 0.24 MPa (35 psi) vs. 0.17 MPa (25 psi) in the initial design.

5.3.2 L3 Distortions from Atmospheric Pressure

A preliminary study of the L3 distortions from atmospheric pressure, was performed and documented in PSDC-300-013-00.

The design of L3 has since slightly changed. After performing the sensitivity analysis, we calculated the final design of the L3 corrector and its cell. Instead of a diameter of 500 mm, we now have a diameter of 554 mm and the flat rim we had on the outside for mounting purposes has disappeared.

As we have seen earlier, the introduction of the elastomer and the contact elements greatly changes the results. We will therefore proceed to the same load case calculation (1 atmosphere on the L3 outer surface), with the new design.

As shown in PSDC-300-013-00, the self-gravity effect is negligible with respect to the atmospheric pressure on the lens, so only the 1 atmosphere pressure on L3A load case will be calculated.

We then obtain the following results:

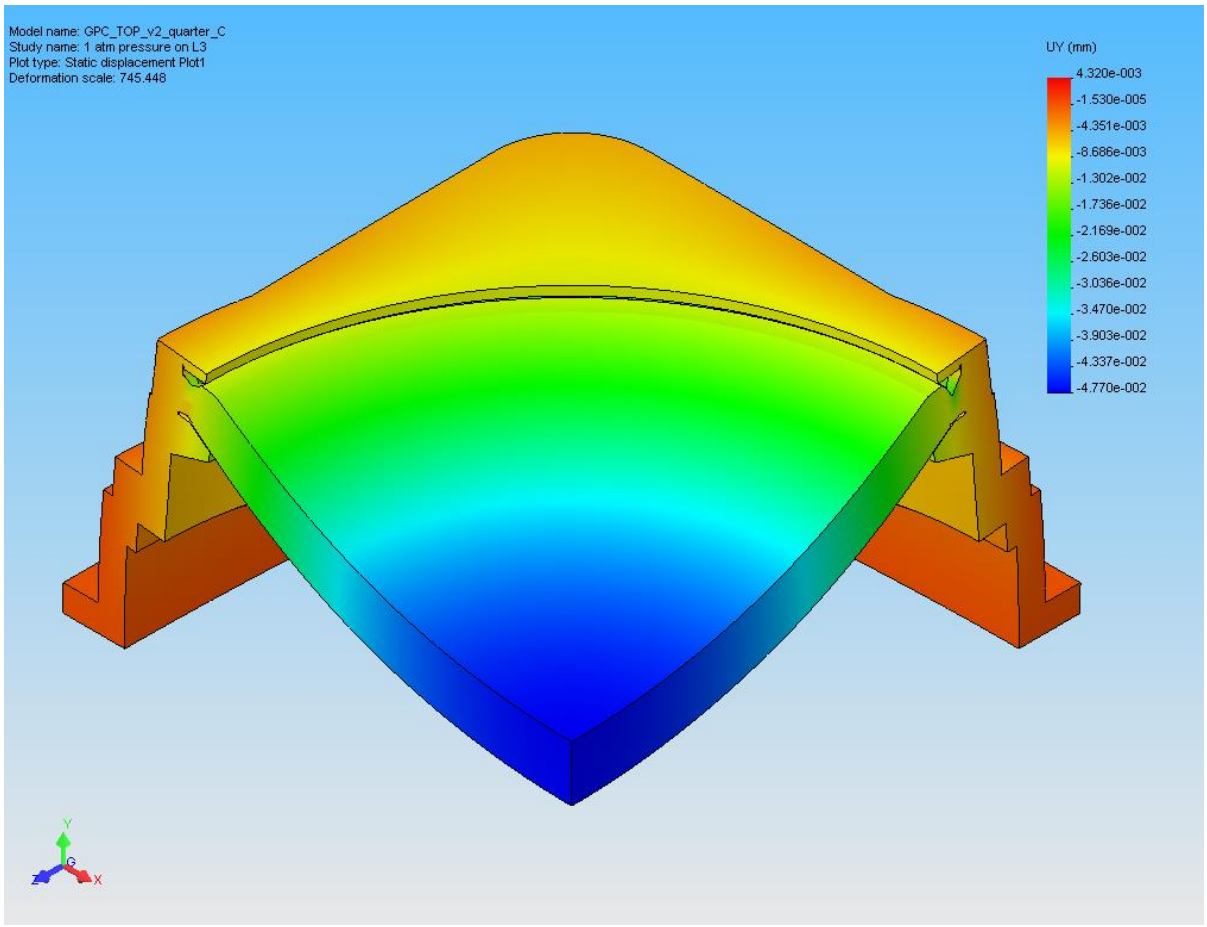

Figure 20. Axial displacements with 1 atmosphere pressure on the upper L3 surface

The maximum axial displacement of L3 obtained in PSDC-300-013-00 was -24 μm (lens pushed down), whereas the maximum displacement obtained here is -48 μm. We observe the same tilt inward of the lens OD as the lens reacts to the applied pressure: the L3A OD shows an inward radial displacement of 11.7 μm, whereas the L3B OD shifts only 5.9 μm.

The distortions obtained with this cell mount represent therefore a surface error of λ/0.0125 (λ=0.61 μm) instead of the λ/0.025 obtained in PSDC-300-013-00, exactly twice as large.

As discussed previously in PSDC-300-013-00, another concern is the failure of the Dewar window. The most appropriate standard of glass strength for failure analysis is the glass tensile strength. The value for Fused Silica is 500 kg/cm^2 (7,112 psi) according to Corning Glass Works. This leads to a minimum FOS (Factor of Safety) in the glass of 14.6, localized on the top chamfer (see Figure 22), where the highest stresses clearly occur (see Figure 21). The preliminary calculation in PSDC-300-013-00, showed a minimum FOS of 5 and concluded that a proper lens mount would highly increase this value.

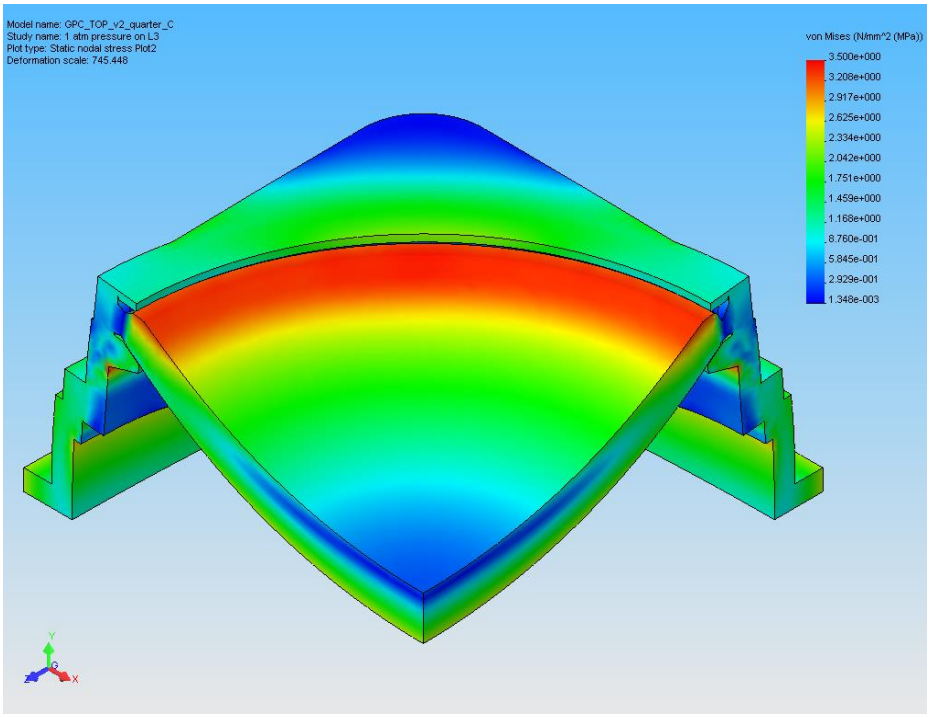

Figure 21. Von Mises Stresses in L3 under 1 atm pressure - Scale modified for visualizing the stresses in the glass

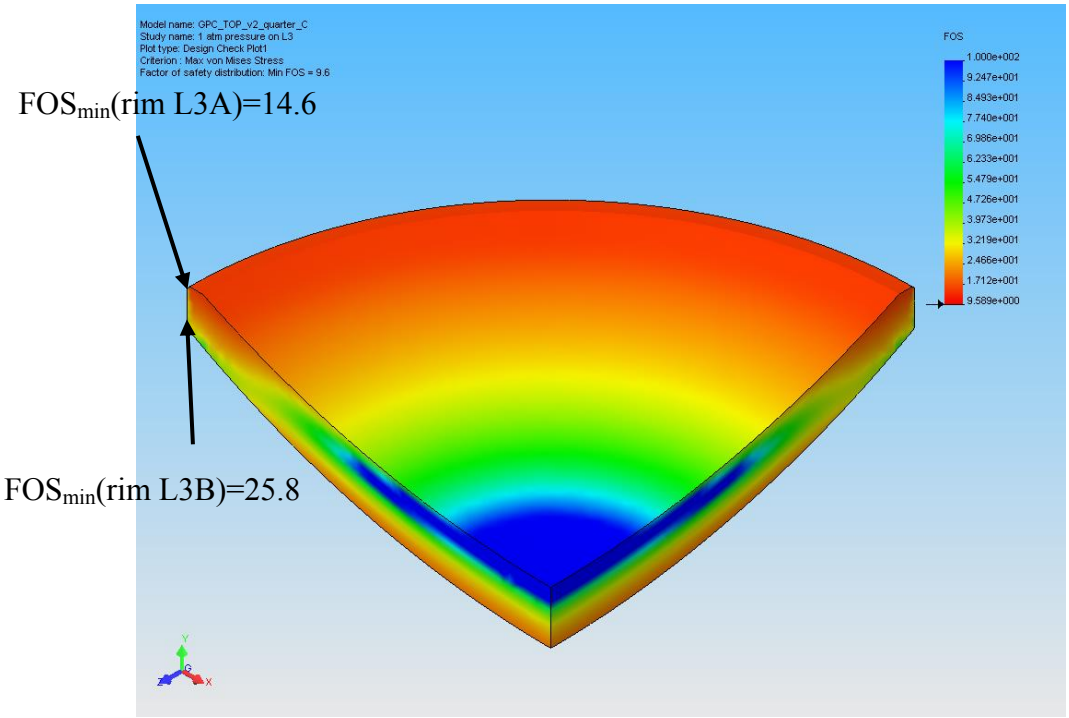

Figure 22. Factor of Safety in L3 (other components occulted)

5.3.3 Combined effects of atmospheric pressure and temperature effect

When combining the effects of temperature and pressure, we obtain the following stress levels:

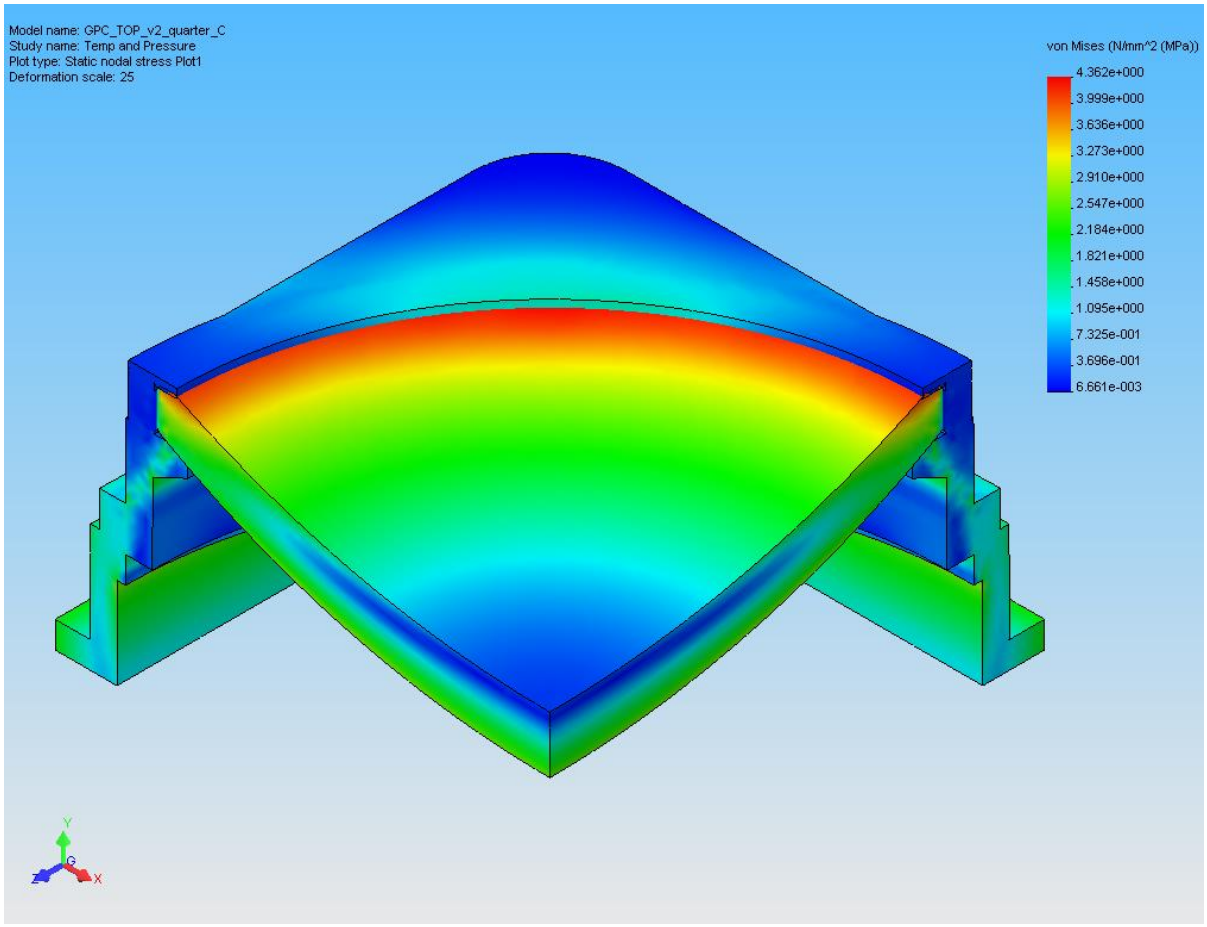

Figure 23. Combined effects of pressure and temperature on L3 stresses

	1 atm pressure on L3A	T = -10 °C	1 atm pressure on L3A and T = -10 °C
Maximum stress in the glass	3.3 MPa [485 psi]	0.24 MPa [35 psi]	4.1 MPa [601 psi]
Axial Displacements at vertices	-47.7 µm (L3A) -47.4 µm (L3B)	-21.6 µm (L3A) -20.2 µm (L3B)	-74.3 µm (L3A) -72.7 µm (L3B)
Axial Displacements of lens perimeter	-9.9 µm (L3A) -10.1 µm (L3B)	-21.9 µm (L3A) -21.0 µm (L3B)	-31.7 µm (L3A) -30.9 µm (L3B)
Radial Displacements of perimeter	11.7 µm (L3A) 5.9 µm (L3B)	10.0 µm (L3A) 9.8 µm (L3B)	24.1 µm (L3A) 16.5 µm (L3B)

Table 12. FEA Results on the L3 corrector

When combining both effects, the results do not add up linearly. Therefore, when a ΔT of 34 °C will occur during operation (1 atm on L3A will apply at the same time), high stresses will be generated in the glass.

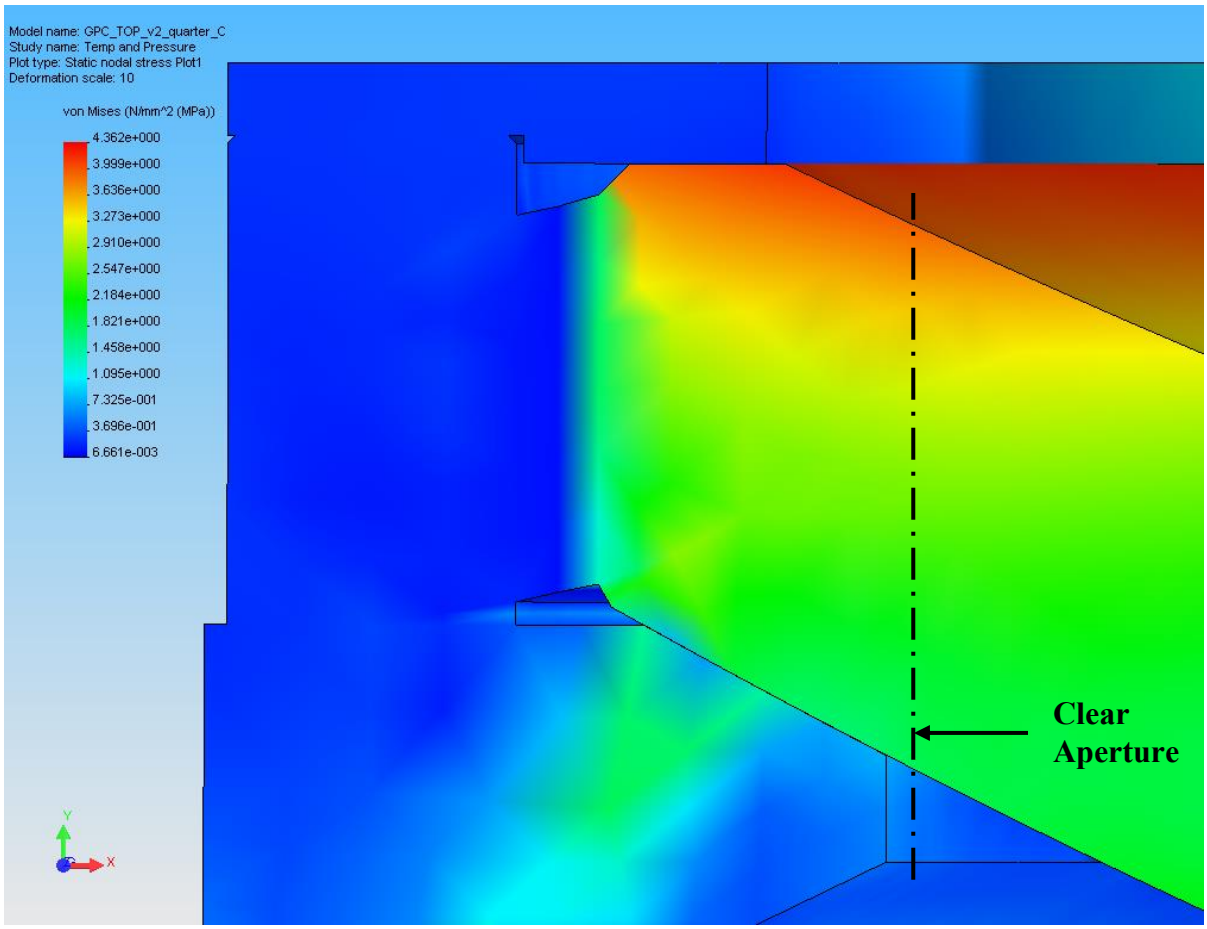

Figure 24. Von Mises Stresses in L3 close to the clear aperture

Close to the clear aperture, stresses are still 4.02 MPa (583 psi) in the glass.

A Zemax analysis would be required.

6 Conclusion

A first important result from the analyses we performed is that the RTV ring shall not reach the bottom metal surface, in order for the RTV to be able to expand and contract freely in that area. We considered a gap of 2 mm, which is more than sufficient for the RTV to expand/bulge.

The studies we performed on all three correctors show that the closed-form equations indeed yield an optimal RTV thickness, from the stress level point of view. The sensitivity studies performed on the RTV thickness show a different behavior for each lens, due to their rather different geometries. The fitted curves obtained from these data enable us to predict the stress levels in the glass for any given RTV thickness within the analyzed range.

For manufacturing purposes, we determine the closest rounded cell radius necessary to approach that optimum RTV thickness and consider manufacturing tolerances on both the lens cell and the lens itself. The resulting RTV thicknesses are presented in Table 13, together with estimated tolerances and stresses, for the definitive correctors design.

	Clear Aperture [mm]	Outer Lens Radius [mm]	Optimal RTV thickness [mm]	Inner Cell Radius [in.]	RTV thickness and tolerances [mm]	Expected stress range [psi]
L1	310.0	328.0	4.512	13.09	4.486±0.254	[41-42]
L2	287.0	305.0	4.195	12.17	4.118 ±0.254	[40-41]
L3	259.0	277.0	7.49	11.2	7.48±0.254	[29-40]

Table 13. RTV Thicknesses and tolerances for the PS-1 correctors (corrector radii increased by about 10 mm w.r.t. the initial studies)

The analyses showed that in the case of the second corrector, the deformation of the lens due to the thermal effect, is more important than the gravity one, by a factor of 50, and the temperature difference generated stresses are 3 times greater than the ones generated by gravity. A Zemax analysis of these distortions generated by gravity will need to be performed.

Comparing to results previously obtained in preliminary studies, we obtain higher despacing of both L2 and L3, due to the introduction of the elastomer and to the contact elements, enabling the glass to slide on the metal, and squeeze the elastomer. But in the case of L3 for instance, the stresses in the glass are lower than in the preliminary studies. The higher stresses obtained for L2 result from the lens shape, even after athermalization.

After analyzing the final L3 design, stresses in L3 due to the temperature difference, can be expected to be slightly higher (10 psi) than first calculated. But as seen, the atmospheric pressure generated stresses are dominating.

The lens mounts design for all three correctors will be made according to the results obtained in these studies, and taking into account the specifics detailed in PSDC-300-019-DR.

7 Appendix

7.1 Athermalization (example of L1)

The following study is based on "Athermal design of nearly incompressible bonds": by Doyle et al.

When considering uniform temperature changes, a simple RTV ring shape is sufficient. The athermalization in the radial direction needs then to be performed considering the optics radius. It is stated that the proper sizing of the thickness is critical for high shape factor RTV bonds, in order not only to minimize the stress concentrations in the glass, but mainly to minimize the radius of curvature changes. Whereas the other corrector lenses in PS1 present low shape factors, L1 due to its large thickness presents a shape factor of about 22.

The first closed-formed equation yielding the athermal RTV thickness is given by Bayer:

Bayer: $$t_{bond} = R_{optic} \frac{\alpha_{cell} - \alpha_{optic}}{\alpha^*_{bond} - \alpha_{cell}}$$

Where α^*_{bond} is the effective CTE

Three references give us an indication on the value of this effective CTE. Fata and Fabricant and Mast et al. both consider an RTV 560 from GE Silicones. Their test results are presented in Figure 25. They also both refer to the measurements performed by Lobdell on a different RTV ("The effect of shear restraint on the properties of RTV11", *Itek Interoffice Memorandum*, November 13, 1968), even if the results they present differ from one another: see Figure 26.

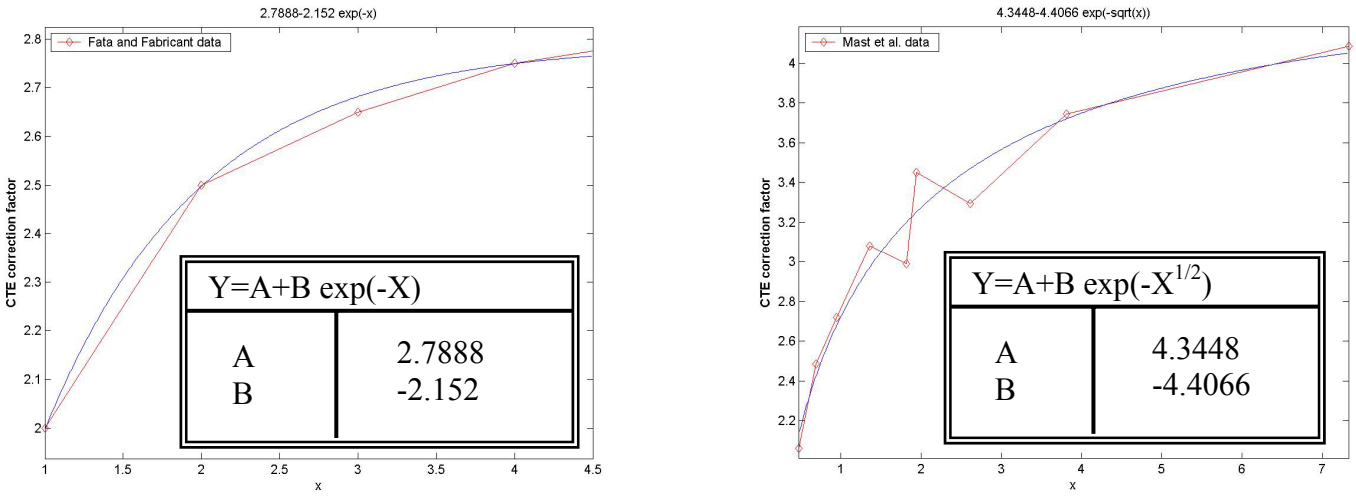

Figure 25. CTE correction factor vs. Shape Factor – Test results for RTV560

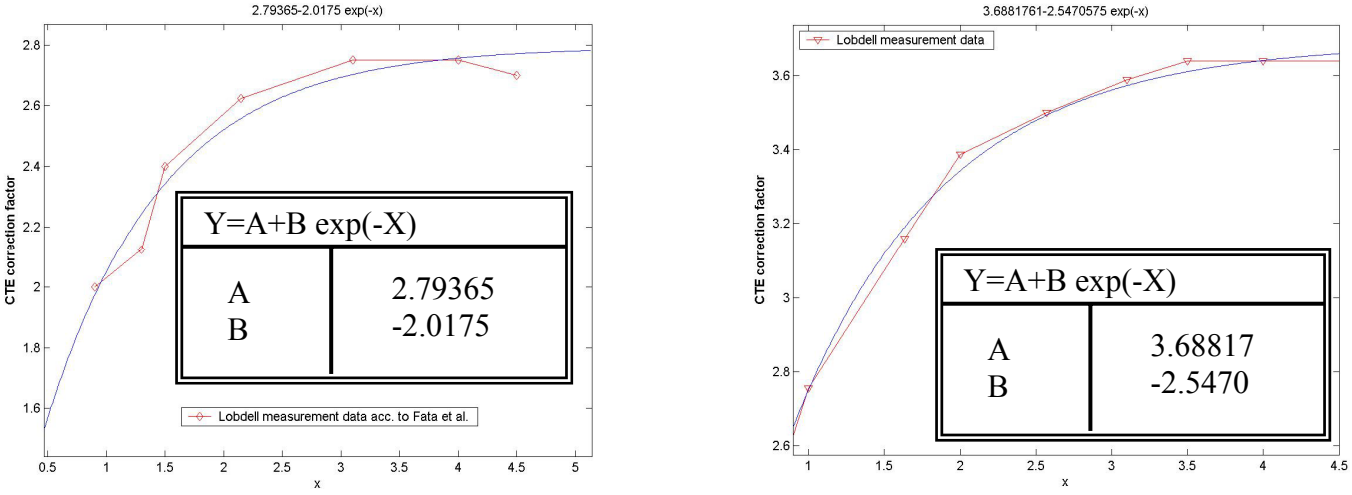

Figure 26. CTE correction factor – Lobdell measurements acc. to Fata and to Mast

Finney refers to a correction factor K_T to account for the relation between the thickness change and shape factor, when submitted to a temperature change. For low shape factor, this factor tends to 1, but for a shape factor of about 22, it tends to 2.9.

Source	CTE correction factor
Fata and Fabricant	2.79
Mast et al.*	4.3037
Lobdell acc. to Fata et al.	3.688
Lobdell acc. to Mast et. al	2.7936
Finney	2.9

Table 14. CTE correction factor

* the interpolation has been performed on the test results, without considering the errors indicated by the author

The other two closed-form equations given by Doyle are:

Deluzio:
$$t_{bond} = R_{optic}\frac{1-\nu_{bond}}{1+\nu_{bond}}\left(\frac{\alpha_{cell}-\alpha_{optic}}{\left(\alpha_{bond}-\alpha_{optic}\right)-\frac{\left(7-6\nu_{bond}\right)\left(\alpha_{cell}-\alpha_{optic}\right)}{4\left(1+\nu_{bond}\right)}}\right)$$

Meunch:
$$t_{bond} = R_{optic}\frac{\left(1-\nu_{bond}\right)\left(\alpha_{cell}-\alpha_{optic}\right)}{\alpha_{bond}-\alpha_{cell}+\nu_{bond}\left(\alpha_{bond}-\alpha_{optic}\right)}$$

The RTV thickness for an athermal design shall therefore be:

Equation		Athermal Bond Thickness [mm]
Bayer	Correction factor from Fata	4.622
	Correction factor from Mast	2.98
	Correction factor from Lobdell acc. to Fata	3.483
	Correction factor from Lobdell acc. to Mast	4.616
	Correction factor from Finney	**4.444**
Deluzio		**4.3740**
Meunch		**4.3739**

Table 15. Athermal bond thickness for the PS-1 L1 corrector

It is therefore clear that the best approximation of the CTE correction factor as function of the shape factor is given by Finney, and then by the Lobdell measurements according to Mast et al. and finally the measurements performed by Fata et al. The measurements performed by Mast et al. are not so good and the Lobdell measurements presented by Fata et al. do not match the ones presented by Mast et al.

Deluzio and Meunch give almost the same value, which was to be expected as both equations are equivalent for $\nu=0.5$. For the future design of the PS-1 correctors mounts, we will use the Deluzio formula.

7.2 Potting

7.2.1 Potting Process

1. **Axial and radial alignment**

   See PSDC-300-019-DR: axial machined pads and radial positioning studs.

2. **Preparation**

   In order to obtain a string adhesion to adjacent surfaces, these ones must be previously cleaned with a primer (Dow corning 1201 RTV Primer)

3. **Mixing**

   RTV 3112 is a two part compound which requires mixing. The recommended mixing ratio is 10:1 base to catalyst. Two different catalysts could be used: catalysts 1 and S. Catalyst S stands for standard rate. Catalyst 1 is the same as catalyst S but with no corrosion inhibitor. Both catalysts yield a curing time between 6 and 12 hours, depending on the mixing ratio.

   Either hand mixing or mechanical mixing is satisfactory. With either method, care should be taken not to whip large amounts of air into the mixture. If vacuum deairing is planned, the container should be no more than one-half full to allow for the expansion during the vacuum cycle.

4. **Degassing** ("Vacuum deairing" according to http://www.dowcorning.com)

   According to Dow Corning, when vacuum deairing is necessary, it should be done first in the mixing container, with at least 28 mm of mercury, until most bubbling has ceased. And they recommend repeating the procedure after the mixture has been poured in place, for better results.

   For the DEIMOS camera, they proceeded to degassing after preparing the mixture, placing the RTV in a bell jar and drawing down to an absolute pressure of 25 mm of mercury (they used RTV 560 from GE Silicones), until the mixture stopped frothing. They quote that the volume increased by a factor of 4 to 5. *Dow Corning states a value of volume expansion (between 25 °C and 150 °C) of* 885×10^{-6} *cc/cc/°C.*

5. **Injection**

   Again, according to the DEIMOS experience, the dispensing of the liquid RTV, neatly and evenly is challenging. They opted for a 60 cc syringe, placed in a specially designed holder. This holder has a threaded plunger which advances as a screw is turned (a manual procedure is tiresome and leads to uneven results). The holder is maintained in place in a stationary jig, so that the tip does not move with respect to the lens and cell. The cell is mounted on a motorized rotary table which turns the cell at a constant speed. The RTV thus leaves the tip in a thick stream and falls into the gap. The flow rate needs to be kept low enough for the RTV to fall straight down into the gap, otherwise there is a risk for the RTV stream to hit the walls of the gap and generate an uneven result.

We consider two different approaches for the injection of the RTV between glass and cell: see Figure 27 and Figure 28. This only applies to the L1 and L2 correctors. The L3 corrector cell, as described in PSDC-300-019-DR, will be a split cell, and can use a removable sleeve, unlike the other two correctors.

For the centering of both L1 and L2 within their respective cells, some positioning studs are intended to be used and removed after the RTV has cured. For this, a release agent may be needed on the studs to aid their removal.

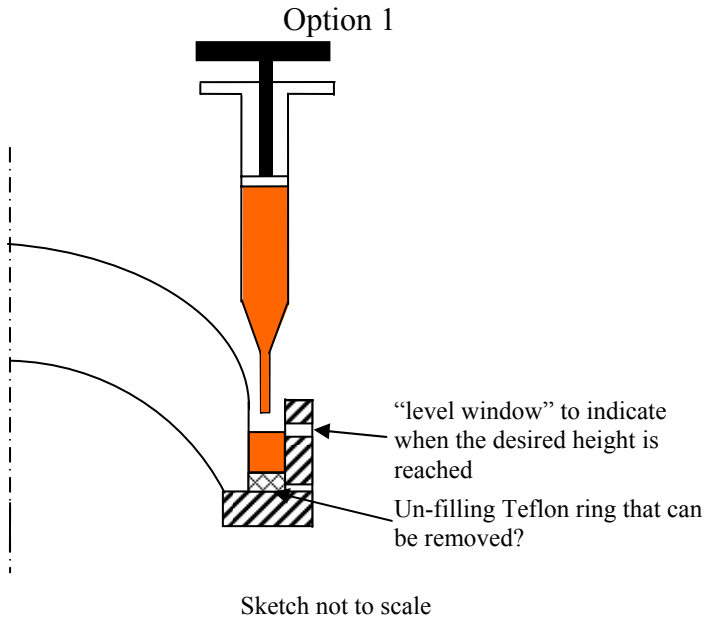

Figure 27. Option 1 of the injection strategy

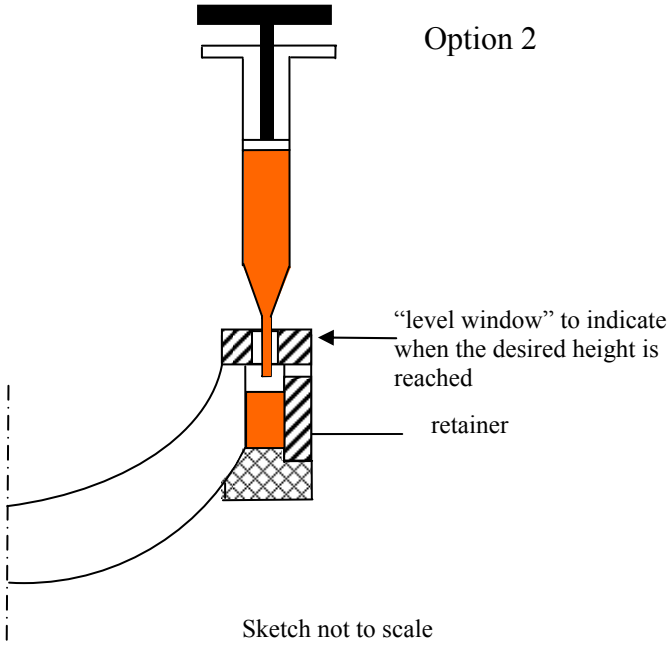

Figure 28. Option 2 of the injection strategy: lens upside down

For option 2, the lens could be axially supported during the potting process.

The viscosity value given by Dow Corning is 280 poise at 25 °C.

6. **Curing**
   The curing rate is function of both temperature and humidity. Curing time will increase for temperatures below 23 °C, and exposure to high humidity will tend to decrease it. For the standard mixture ratio 10:1, the curing time is estimated to be of 8 hours, with an approximate working time of an hour.

7.2.2 Quantities needed

Dow Corning specifies on its product data sheet, that the RTV 3112 base is available in 0.1 lb (0.45 kg), 9 lb (4.1 kg), 40 lb (18.2 kg) and 400 lb (182 kg) containers. The catalysts S and 1 are supplied in 0.1 lb (45g) tubes and 0.9 lb (0.41 kg) and 4 lb (1.82 kg) containers. Catalyst 1 is also available in 40 lb (18.2 kg) containers.

The current design leads to an estimated volume of RTV of 2.05 dm^3 (considering potting for 6 filters as well as for the three correctors). Therefore considering that during the vacuum de-airing the volume is multiplied by about 2, we would only need 1.03 dm^3. Considering a density of 1.3 kg/ dm^3, we would need 1.33 kg (2.94 lb) of RTV mixture. If we consider the recommended mixture ratio of 10:1, this translates in 1.2 kg (2.64 lb) of RTV base and 0.13 kg (0.29 lb) of catalyst.

We would therefore need either:

- 3 containers of 0.1 lb (0.45 kg) of RTV 3112 base, and 3 tubes of 0.1 lb (45 g) of catalyst S or 1.
- 1 container of 9 lb (4.1 kg) of RTV 3112 base, and 1 tube of 0.9 lb (0.41 kg) of catalyst

7.2.3 Storage and shelf life

Still according to the Dow Corning data sheet, the shelf life of RTV 3112 is 24 months from date of manufacture, and the shelf life of catalysts S is 24 months from date of manufacture when stored in original, unopened containers at 23 °C (73 °F).

We obtained samples of RTV 3112 and catalyst S and will perform some potting tests on a small lens.